Report Number
TM-62-1

Diffuser Studies with Single- and Two-Phase Flows

by

G. R. Schneiter

Contract N onr 1100 (07)

April 1962

JET PROPULSION CENTER
PURDUE UNIVERSITY

SCHOOL OF MECHANICAL ENGINEERING
LAFAYETTE, INDIANA

PURDUE UNIVERSITY

AND

PURDUE RESEARCH FOUNDATION
Lafayette, Indiana

Report No. TM-62-1

Technical Memorandum

DIFFUSER STUDIES WITH SINGLE- AND TWO-PHASE FLOWS

G. R. Schneiter

Approved by: M. J. Zucrow

M. J. Zucrow
Atkins Professor of
Engineering

Contract N onr 1100(07)

Jet Propulsion Center
Purdue University

April 1962

ACKNOWLEDGMENTS

The research reported herein was sponsored by the Office of Naval Research, Contract N onr 1100(07). Reproduction of this document in whole or in part is permitted for any purpose of the United States Government.

The author wishes to express his gratitude to Dr. M. J. Zucrow, and also to Dr. B. A. Reese and Dr. C. F. Warner, for their valuable suggestions and recommendations throughout the course of this research program and during the writing of the report.

Mr. Donald Crabtree deserves special recognition for his unselfish instruction, guidance, and advice. Gratitude is also expressed to Mr. Bruce Landeck for his capable assistance during the course of the experimental investigation; to Mr. Bill Timmons for his help with the construction of the experimental apparatus; and to Mrs. Jean Patterson for her willing secretarial assistance.

Acknowledgment is also given to the National Science Foundation for its financial support.

TABLE OF CONTENTS

Page

LIST OF TABLES

LIST OF ILLUSTRATIONS

Figure | Page

ABSTRACT

This report discusses an experimental investigation of two problems of diffuser flow which are encountered in a gas-driven jet pump. The first was concerned with determining the feasibility of diffusing a free jet of liquid, as contrasted with a stream of liquid flowing into a diffuser under "connected-pipe" conditions. The second problem was concerned with determining the effect of entrained gas in the flowing liquid upon the diffusion process. In all of the experiments, conical diffusers were employed with water and air as the working fluids.

In the free-jet experiments a nozzle was employed for furnishing a free jet of water which was directed into a specially designed inlet to a diffuser. Determinations were made of (1) the fraction of the jet which actually flowed into and through the diffuser, and (2) the fraction of the original kinetic energy of the captured jet that was converted into static pressure rise. The variables in these experiments were the liquid flow rate, the distance between the nozzle and the diffuser inlet, the ratio of the diameter of the jet to the diameter of the diffuser inlet, the configuration of the diffuser inlet, and the diffuser back pressure.

It was found that up to 86.5 per cent of the kinetic energy of the free jet could be recovered by employing the proper type and size of diffuser inlet, with the appropriate back pressure. The experiments

indicated that the flow rate and the distance from the nozzle exit to the diffuser inlet had little effect on the energy recovery.

The gas entrainment experiments were conducted in a "connected-pipe" system with a two-phase mixture of air and water; the velocity of the two-phase mixture entering the diffuser was maintained constant. Determinations were made of the effect of (1) varying the amount of gas entrained in the liquid, and (2) varying the static pressure at the diffuser inlet, upon the diffuser pressure recovery.

The experiments indicated that when a gas is entrained in a liquid being diffused, the pressure recovery of the diffuser is reduced, the amount of reduction depending on the volume of entrained air and the static pressure at the throat of the diffuser. A theoretical analysis indicates that the reduction in pressure recovery due to gas entrainment should become smaller as the entrance velocity to the diffuser is increased. The experiments indicated, however, the possibility that compressibility effects may seriously reduce the pressure recovery for high velocity, two-phase flow in a diffuser.

1 INTRODUCTION

The ability of the diffuser in a gas-driven jet pump to capture and diffuse efficiently the high velocity stream of liquid directed toward it is of great importance to the overall momentum recovery of the pump. The momentum-recovery factor K of a gas-driven jet pump, as defined by Elliott (3),* is equal to

$$K = K_1 K_2 K_3 K_4 \sqrt{K_d} \qquad (1\text{-}1)$$

where K_1 = the velocity-recovery factor of the drive nozzle;

K_2 = the momentum-recovery factor of the mixer;

K_3 = the mass-recovery factor of the separator;

K_4 = the velocity-recovery factor of the separator; and

K_d = the efficiency of the diffuser.

Equation 1-1 shows that the momentum-recovery factor K is proportional to K_3, which is the portion of the flowing liquid that actually enters the diffuser, and increases with the square root of K_d, which is the portion of the dynamic pressure of the liquid entering the diffuser that is converted into static pressure.

Certain problems are encountered in diffusing a jet of liquid in the diffuser of a jet pump that do not exist in conventional

---

* Numbers in parentheses refer to references appearing at the end of the report.

diffuser applications; that is, "connected-pipe" diffusion processes. Two problems peculiar to the diffusion process in a gas-driven jet pump are discussed herein.

One problem arises from the fact that the liquid to be diffused enters the diffuser as either a free jet or a film, depending on the type of jet pump configuration employed. In most reported applications of diffusers, on the other hand, the fluid enters the diffuser through a duct connected to the diffuser; that is, under "connected-pipe" conditions. Figure 1 illustrates schematically the flow of a liquid through a conical diffuser with (a) free-jet, and (b) connected-pipe entrance conditions.

Consequently, one phase of the investigation was concerned with the flow of a free jet of a liquid into and through a conical diffuser. Studies were made of the effect of the ratio of the diameter of the jet to the diameter of the inlet of the diffuser, and the effect of the shape of the diffuser inlet.

If the separation of the drive gas from the liquid in the separator of a jet pump is imperfect, a two-phase mixture of gas and liquid enters the diffuser (3). It was found that the amount of gas entrained in the liquid affects the pressure recovery characteristics of the diffuser. Accordingly, a study was made of the effect of gas entrainment upon the performance of a conical diffuser. In that connection the effects of the static pressure at the diffuser inlet and the amount of entrained gas upon the diffuser pressure recovery were investigated.

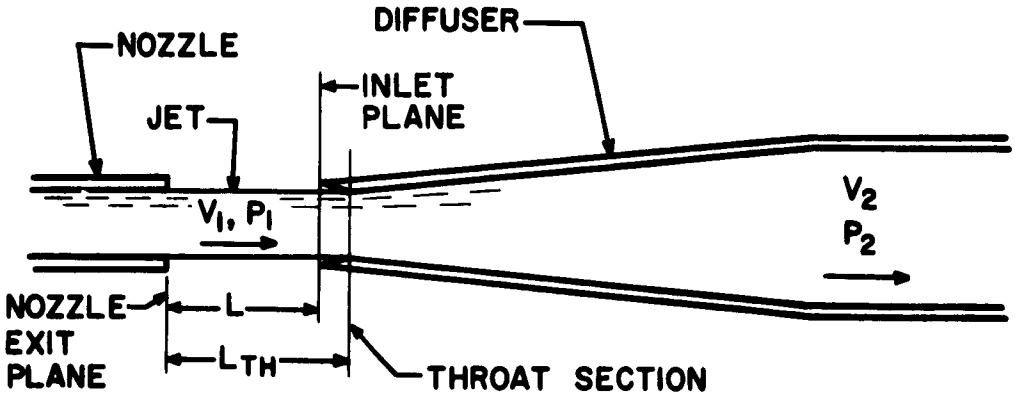

D_N = EXIT DIAMETER OF NOZZLE
D_{ST} = DIAMETER OF FREE JET AT DISTANCE L_{TH}
D_{TH} = DIAMETER OF THROAT OF DIFFUSER

(a) FREE-JET ENTRANCE

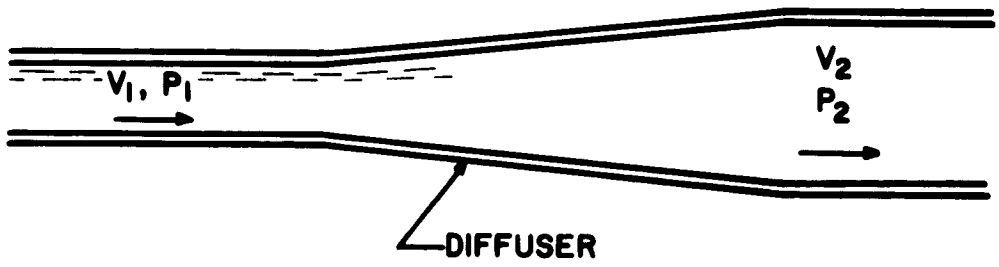

(b) CONNECTED-PIPE ENTRANCE

Fig. 1 Conditions of Entrance for the Flow of a Liquid Through a Conical Diffuser

The experiments were performed using water and air as the working fluids, with diffuser inlet velocities ranging from 70 to 220 fps. A conical diffuser with an inlet diameter of 0.400 in., an exit diameter of 1.200 in., and a total angle of divergence of 7°, discharging into a plenum chamber, was employed in all of the experiments.

2 REVIEW OF THE LITERATURE

A study of the literature pertinent to diffusers revealed no references which were directly applicable to the two specific diffusion problems mentioned in the Introduction. Considerable experimental and analytical work has been reported, however, concerning flow of liquids through diffusers, and also the flow of two-phase fluids.

Gibson's investigations of the flow of water through diverging passages (4) constitutes the first significant work performed on diffusion flow. He found that the optimum pressure recovery for a conical diffuser occurred when the total angle of divergence of the diffuser was 6°. In his experiments the effect of the entrance velocity was negligible over a range of values from 1.83 to 21 fps. The inlet diameters of the diffusers employed were from 0.5 to 2 in.

A recent paper by Kline, Abbott, and Fox (6) correlates the findings of previous investigators of diffusers so that the flow regime to be expected for a given geometry can be predicted. These correlations include both the flow of liquids and gases. It is also possible, for a diffuser of given length, to predict the angle of divergence giving the optimum pressure recovery. The actual values for the pressure recoveries obtainable with various geometries cannot, however, be predicted accurately, because of the large number of variables involved.

The range of Reynolds' numbers in the experiments reported herein falls within that of the experiments reported in Reference 6.

Robertson and Ross (10) and Peters (9) discuss the effect of the entrance conditions upon diffuser performance; their work primarily concerns the effect of boundary layer development on pressure recovery. Robertson and Ross used water as a working fluid, whereas Peters worked with air. They both found that when a boundary layer existed at the entrance to a diffuser, the pressure recovery of the diffuser was reduced; and the thicker the boundary layer, the larger was the reduction in pressure recovery. According to Robertson and Ross the effect of the entering boundary layer upon the pressure recovery was of the same order as the effect of the angle of divergence of the diffuser.

Chenoweth and Martin (1) present a method for calculating the pressure drop of gas-liquid mixtures in horizontal pipes.

3 EXPERIMENTAL RESULTS

All experiments described herein were performed using water and air as the working fluids.

Figure 2 presents a drawing of the basic diffuser apparatus employed in the experiments. A conical diffuser was employed, with an inlet, or throat, diameter of 0.400 in., and an exit diameter of 1.200 in., giving an area ratio of 9 to 1. The total angle of divergence was 7°, which is the angle for the maximum pressure recovery (6). The diverging, or diffusing, section was 6.54 in. long; it was preceded by a rounded, converging nozzle to furnish an approximately uniform velocity distribution at the inlet to the diffuser.

The diffuser discharged into a 6 in. diameter plenum chamber which was 12 in. long; the reduction in the velocity of the fluid was such that its kinetic energy was negligible. The back pressure on the diffuser was varied by adjusting the opening of a valve downstream from the plenum chamber.

In the course of the several investigations, the afore-mentioned basic apparatus was modified as will be noted. A detailed description of the entire apparatus is presented in Reference 11.

3-1 Description of the Free-Jet Experiments

The experimental results presented in Sections 3-2 and 3-3 are

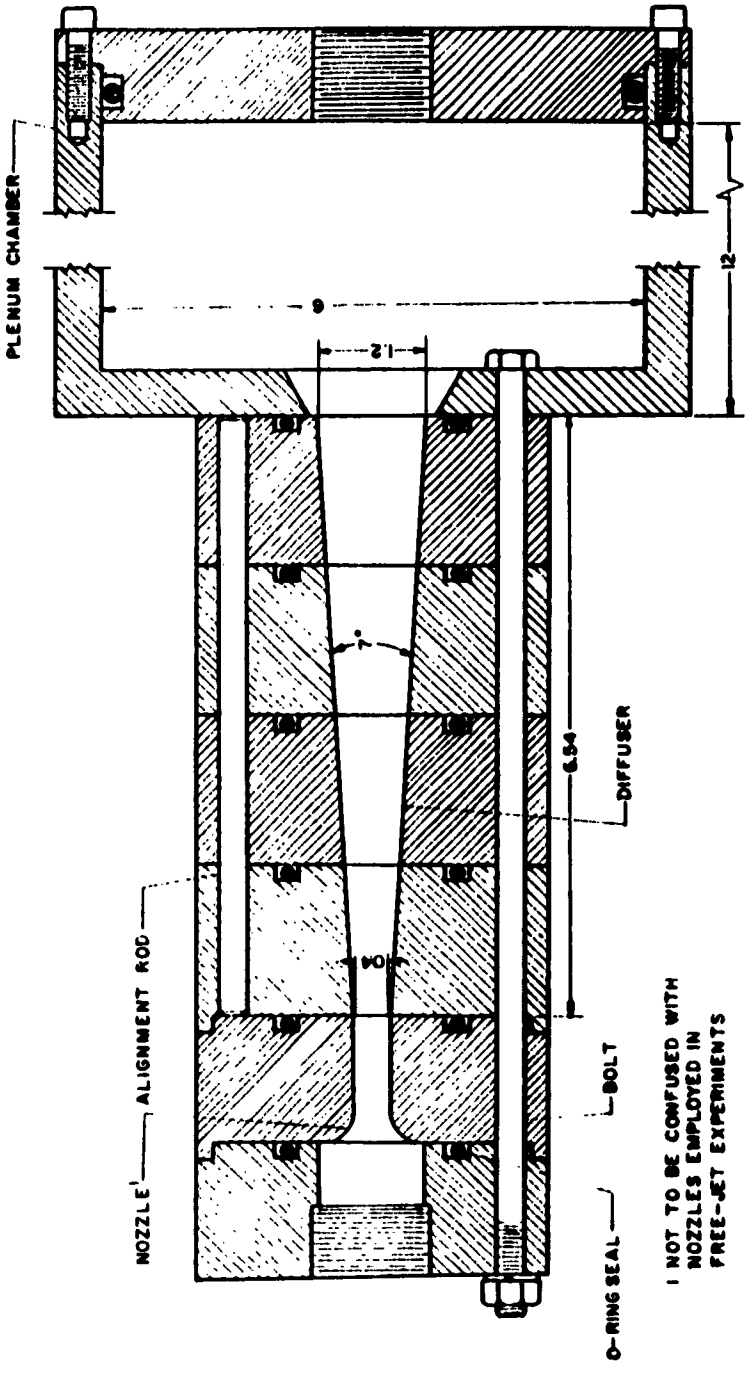

Fig. 2 Basic Diffuser Apparatus (Connected-Pipe Experiments)

based on the experiments conducted with diffusers operating under free-jet entrance conditions (see Figure 1). For convenience of discussion the free-jet experiments will be segregated into Series I and Series II.

3-1.1 Free-Jet Experiments - Series I. The Series I experiments were of an exploratory nature; the objective being the determination of the parameters having the greatest effect on the overall energy recovery characteristics of a diffuser operating under free-jet entrance conditions. The experimental program was conducted in two parts, denoted as Series I-a and Series I-b. The Series I experiments are discussed in Section 3-2.

3-1.2 Free-Jet Experiments - Series II. These free-jet experiments were a refinement of the method of experimentation that appeared most promising according to the experience obtained in conducting the Series I experiments. In the Series II experiments, the variables which had little effect on the energy recovery of the diffuser in the Series I experiments were held constant. Thus the effects of the pertinent variables were isolated, and then investigated individually. The Series II experiments are discussed in Section 3-3.

3-1.3 Apparatus for the Free-Jet Experiments. Two additional pieces of apparatus were required for conducting the free-jet experiments; (1) a nozzle for supplying the free jet of liquid, and (2) an appropriate inlet to the diffuser.

Brief descriptions of the nozzles and inlets employed in the free-jet experiments are presented in Sections 3-2 and 3-3. A detailed description of the apparatus is presented in Reference 11.

3-1.4 Variables Investigated in the Free-Jet Experiments. In the experiments, the influences of the following variables were determined:

a. The mass rate of flow of liquid through the nozzle, denoted by M_L. (M_L was varied from M_L = 4 to 12 lb_m per sec.)

b. The distance between the exit plane of the nozzle and the inlet plane of the diffuser, denoted by L and termed the nozzle-diffuser distance. (L was varied from L = 1/8 to 2 in.)

c. The ratio $\theta = D_{ST}/D_{TH}$, where D_{ST} denotes the diameter of the free jet measured at the plane of the throat of the diffuser, and D_{TH} denotes the diameter of the throat of the diffuser (see Figure 1). (θ was varied from θ = 0.72 to 1.41.)

d. The back pressure acting on the diffuser exit section, denoted by P_{PC}.

3-1.5 Performance Criteria for the Free-Jet Diffusers. The overall performance of a free-jet diffuser depends upon the following three performance criteria:

a. The capture efficiency K_{CAP} is defined by

$$K_{CAP} = M_{CAP}/M_L \qquad (3\text{-}1)$$

where M_{CAP} is the liquid flow rate captured by the diffuser, and M_L is the liquid flow rate leaving the nozzle.

b. The pressure recovery factor K_P is defined by

$$K_P = P_{PC} / \overline{P_{DYN}} \tag{3-2}$$

where P_{PC} is the back pressure acting on the diffuser, and $\overline{P_{DYN}}$ is the mean dynamic pressure of the free jet. $\overline{P_{DYN}}$ is defined by

$$\overline{P_{DYN}} = \frac{1}{A} \int_A P_{DYN} \, dA \tag{3-3}$$

where A is the cross-sectional area of the jet at any given plane perpendicular to the axis of the jet, and

$$P_{DYN} = \frac{1}{2} \rho_L V^2 \tag{3-4}$$

is the dynamic pressure at any point in that plane. (In the Series I experiments $\overline{P_{DYN}}$ was computed on the basis that the flow at the exit of the nozzle was substantially one-dimensional.)

c. The overall efficiency K_O is defined by

$$K_O = K_{CAP} K_P \tag{3-5}$$

3-2 Series I Free-Jet Experiments

The object of these preliminary experiments with free-jet diffusers was to determine the influences of the parameters listed in Sub-section 3-1.4 on the performance of free-jet diffusers. For convenience of discussion the Series I free-jet experiments are divided into two different series of experiments, denoted as Series I-a and Series I-b.

3-2.1 Series I-a Free-Jet Experiments. In these experiments both the mass rate of flow M_L and the distance L, the distance between the exit plane of the nozzle and the inlet plane of the diffuser (see Figure 1) were varied. The flow rates investigated were M_L = 4, 6, 8, 10, and 12 lb_m per sec, and the nozzle-inlet distances studied were L = 1/8, 1/2, 1, 1 1/2, and 2 in. Both a converging-diverging inlet having a 0.400 in. throat diameter, denoted as Inlet A, and a diverging inlet having a 0.600 in. throat diameter, denoted as Inlet B, were employed in conjunction with three nozzles, designated as Nozzle A, Nozzle B, and Nozzle C; the exit diameters of these nozzles were 0.374, 0.406, and 0.438 in., respectively (see Table 1).

Table 1

Nozzles and Diffuser Inlets Employed in the Series I Free-Jet Experiments

Nozzle	Exit Diameter, in.
A	0.374
B	0.406
C	0.438

Inlet	Type	Throat Diameter, in.
A	Converging-Diverging	0.400
B	Diverging	0.600

Reference 11 presents a detailed description of the apparatus employed in the Series I experiments.

All of the afore-mentioned experiments were conducted with the discharge valve downstream from the diffuser held wide open. As a result of that type of operation the flow conditions for a given run determined the value of the back pressure. During an experiment the measured variables were the liquid flow rate M_L, the flow capture rate M_{CAP}, and P_{PC}, the back pressure (in the plenum chamber) in psig.

The performance coefficients calculated from the measurements were the capture efficiency K_{CAP}, the pressure recovery factor K_P, and the overall efficiency K_O; these coefficients are defined by equations 3-1, 3-2, and 3-5, respectively.

Attempts to correlate the data obtained from the Series I-a experiments on the basis of either the ratio of the nozzle exit diameter to the inlet throat diameter, the mass rate of flow M_L, or the mean velocity of the jet $\bar{V}$, were unsuccessful. In general, the results indicated that the smaller the jet diameter, the smaller was the pressure recovery factor K_P and the larger was the capture efficiency K_{CAP}. In most cases M_L or $\bar{V}$ had little influence on the magnitudes of K_{CAP} and K_P. Furthermore, in most of the experiments the nozzle-diffuser distance L appeared to have a negligible effect on the performance coefficients; there were a few cases, however, where L had a considerable influence upon them.

3-2.2 Series I-b Free-Jet Experiments. These experiments were conducted with Nozzles A, B, and C and Inlets A and B. Each nozzle was investigated with the two inlets. In all of the experiments the nozzle-diffuser distance was maintained constant at L = 1/2 in., and

the mass flow rate was held constant at M_L = 6 lb_m per sec. The variable was the back pressure P_{PC}.

Since M_L was constant, the dynamic pressure $\overline{P_{DYN}}$ was also a constant, and it follows from the definition of the pressure recovery factor K_D, that

$$K_P = P_{PC} / \overline{P_{DYN}} \propto \text{constant} \times P_{PC} \qquad (3\text{-}6)$$

Hence, it is apparent that by varying P_{PC} the pressure recovery factor K_P was varied.

From the measurements the capture efficiency K_{CAP}, the pressure recovery factor K_P, and the overall efficiency K_O were readily determined.

Figure 3 presents the overall efficiency K_O as a function of the pressure recovery factor K_P for Nozzles A, B, and C employed in conjunction with Inlet A. Figure 4 presents similar curves for Nozzles A, B, and C with Inlet B. It is apparent from referring to Figures 3 and 4 that for each combination of nozzle and diffuser inlet, there is a value of the pressure recovery factor K_P at which the overall efficiency attains its maximum value. The values of K_P and K_O corresponding to that maximum depend upon the nozzle and diffuser inlet combination.

3-3 Series II Free-Jet Experiments

These experiments were conducted in a manner similar to that employed in the Series I-b experiments. M_L was held constant at 6 lb_m per sec, and the nozzle-diffuser distance was maintained constant at L = 1/4 in.

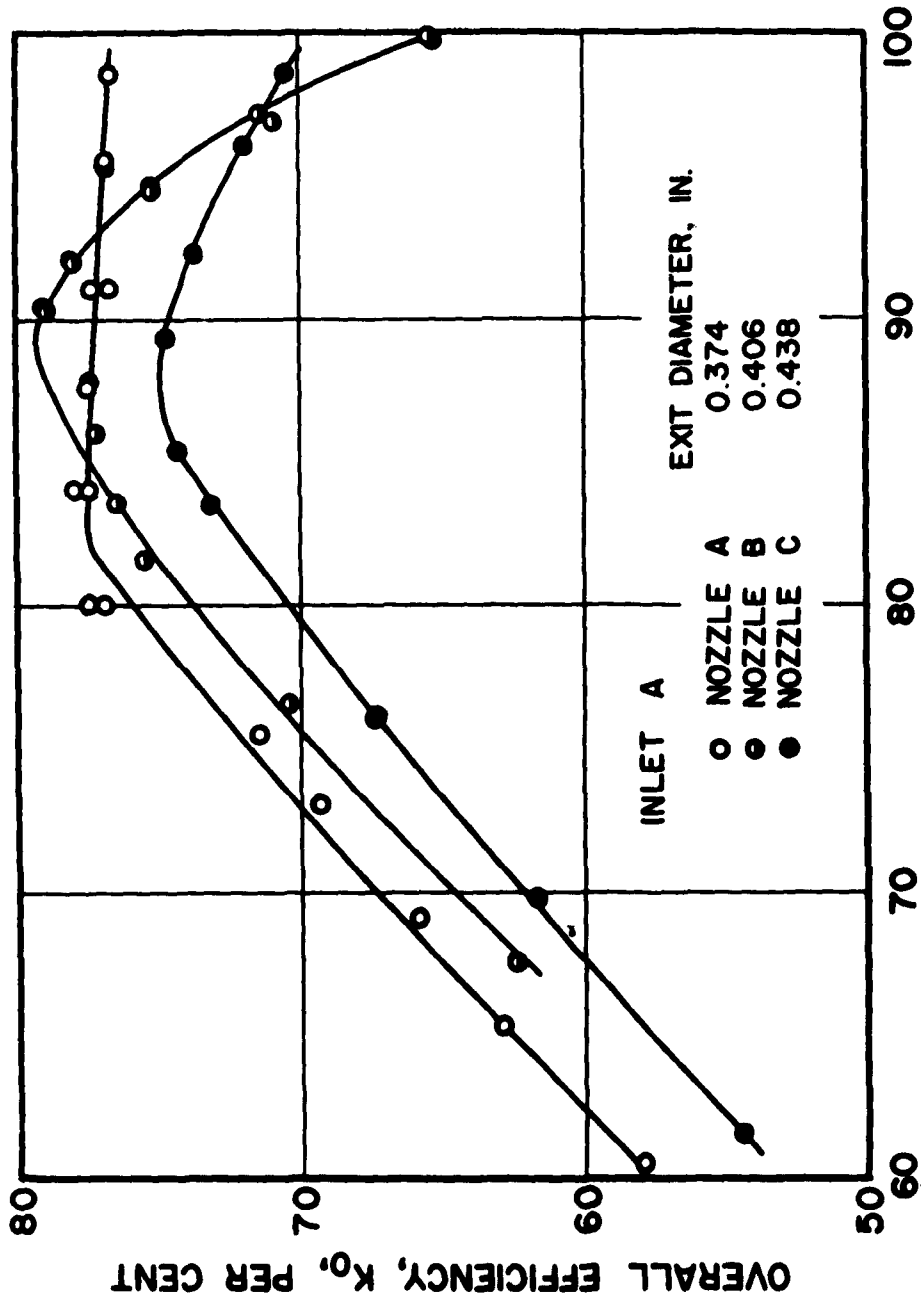

Fig. 3 Overall Efficiency as a Function of the Pressure Recovery Factor for Nozzles A, B, and C and Inlet A

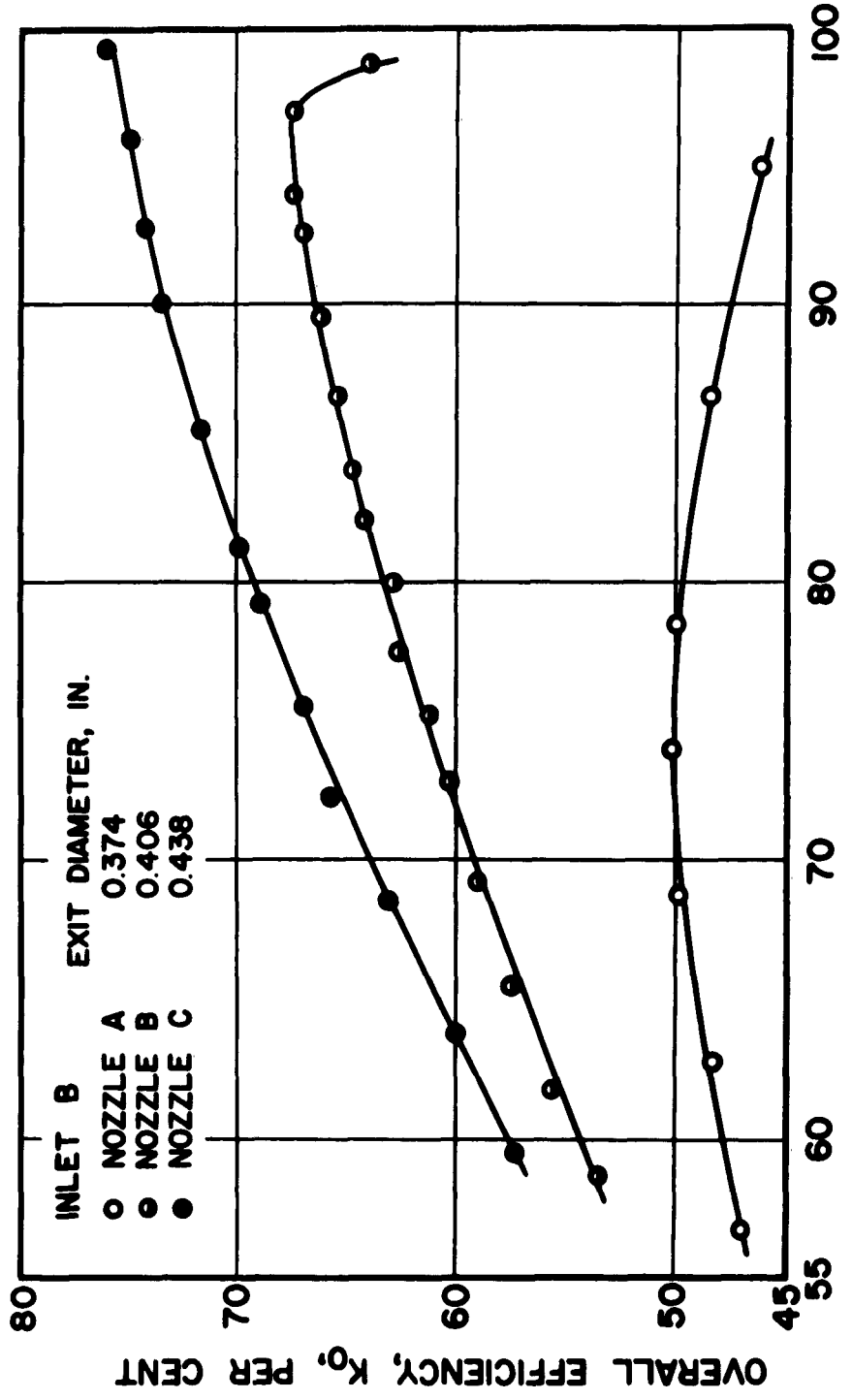

Fig. 4 Overall Efficiency as a Function of the Pressure Recovery Factor for Nozzles A, B, and C and Inlet B

Nozzles of 0.350, 0.402, and 0.452 in. exit diameters, denoted as Nozzles 1, 2, and 3, were each employed in conjunction with three different converging-diverging inlets, denoted as Inlets C1, C2, and C3, and three different diverging inlets, denoted as Inlets D1, D2, and D3. Table 2 presents the exit diameters of Nozzles 1, 2, and 3, and the throat diameters of the afore-mentioned inlets.

Table 2

Nozzles and Diffuser Inlets Employed in the Series II Free-Jet Experiments

Nozzle	Exit Diameter, in.
1	0.350
2	0.402
3	0.452

Inlet	Type	Throat Diameter, in.
C1	Converging-Diverging	0.332
C2	Converging-Diverging	0.415
C3	Converging-Diverging	0.500
D1	Diverging	0.332
D2	Diverging	0.415
D3	Diverging	0.500

Figure 5 illustrates the configurations of the nozzles and the inlets employed in the Series II free-jet experiments. A typical converging-diverging inlet is shown in Figure 5; the diverging inlets

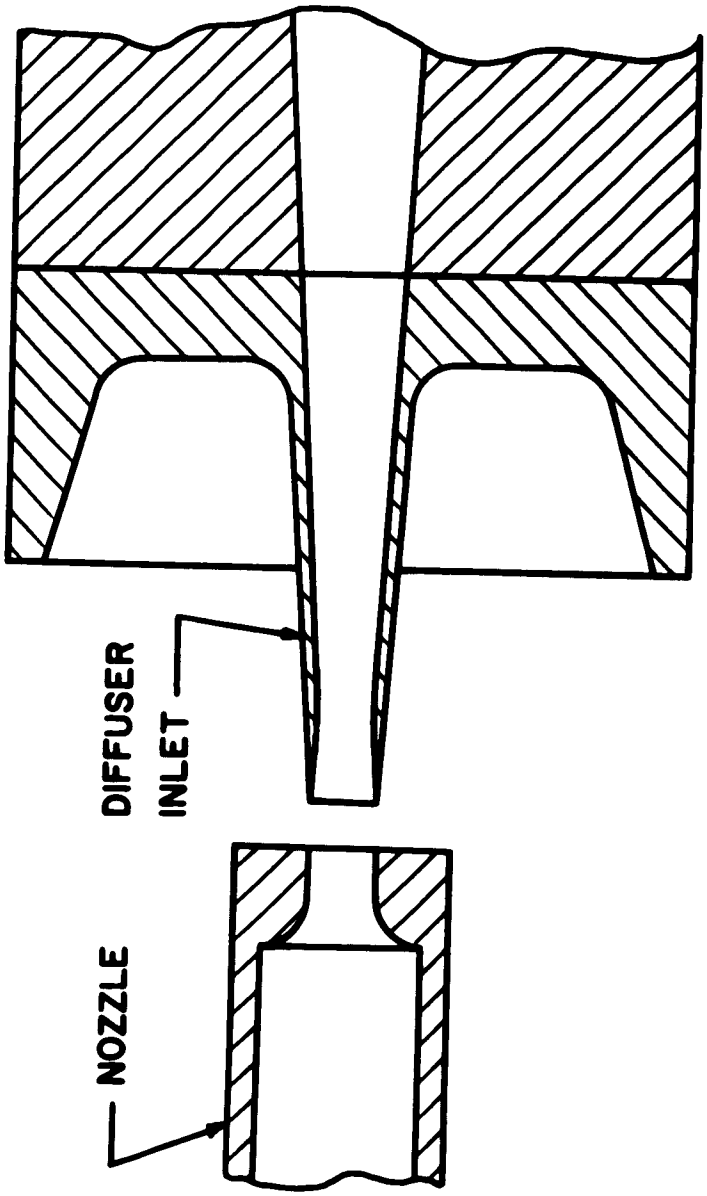

Fig. 5 Typical Nozzle and Inlet Employed in the Series II Free-Jet Experiments

were fabricated by cutting off the converging portions of the converging-diverging inlets. Figure 6 is a photograph of Nozzle 2 and Inlet C1, in position for the free-jet experiments; the collar holds the nozzle and the inlet in the desired positions relative to each other.

A detailed description of the experimental apparatus employed in the Series II free-jet experiments is presented in Reference 11.

By employing all of the possible combinations of nozzles and diffuser inlets, nine different values of the ratio of the free-jet diameter to the diffuser throat diameter, hereafter called the jet-inlet diameter ratio θ, were investigated for each of the converging-diverging, and the diverging inlets. The method employed for computing the diameters of the free jets employed in these experiments is described in Appendix B. Table 3(a) presents the values of θ for the nine nozzle-diffuser inlet combinations for the converging-diverging diffuser inlets; Table 3(b) presents similar information for diffusers employing diverging inlets. Appendix C presents the method of determining the kinetic energies associated with the free jets of liquid discharged from Nozzles 1, 2, and 3.

In all cases the back pressure P_{PC} was varied so that the pressure recovery factor K_P varied from approximately 50 to 100 per cent.

Figure 7 presents the overall efficiency K_O as a function of the pressure recovery factor K_P for Nozzles 1, 2, and 3 employed in conjunction with diffuser Inlets C1, C2, and C3, with the jet-inlet diameter ratio θ as a parameter. Figure 8 presents similar curves for Nozzles 1, 2, and 3 with diffuser Inlets D1, D2, and D3.

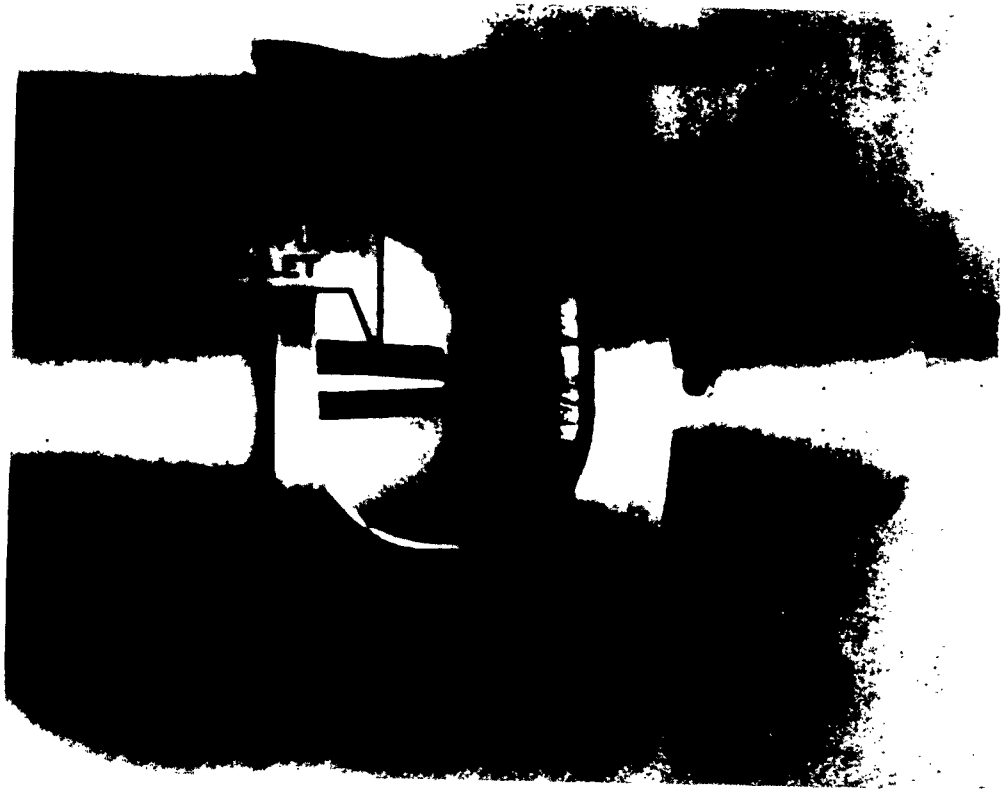

Fig. 6 Diffuser Inlet, Collar, and Nozzle as Employed in the Series II Free-Jet Experiments

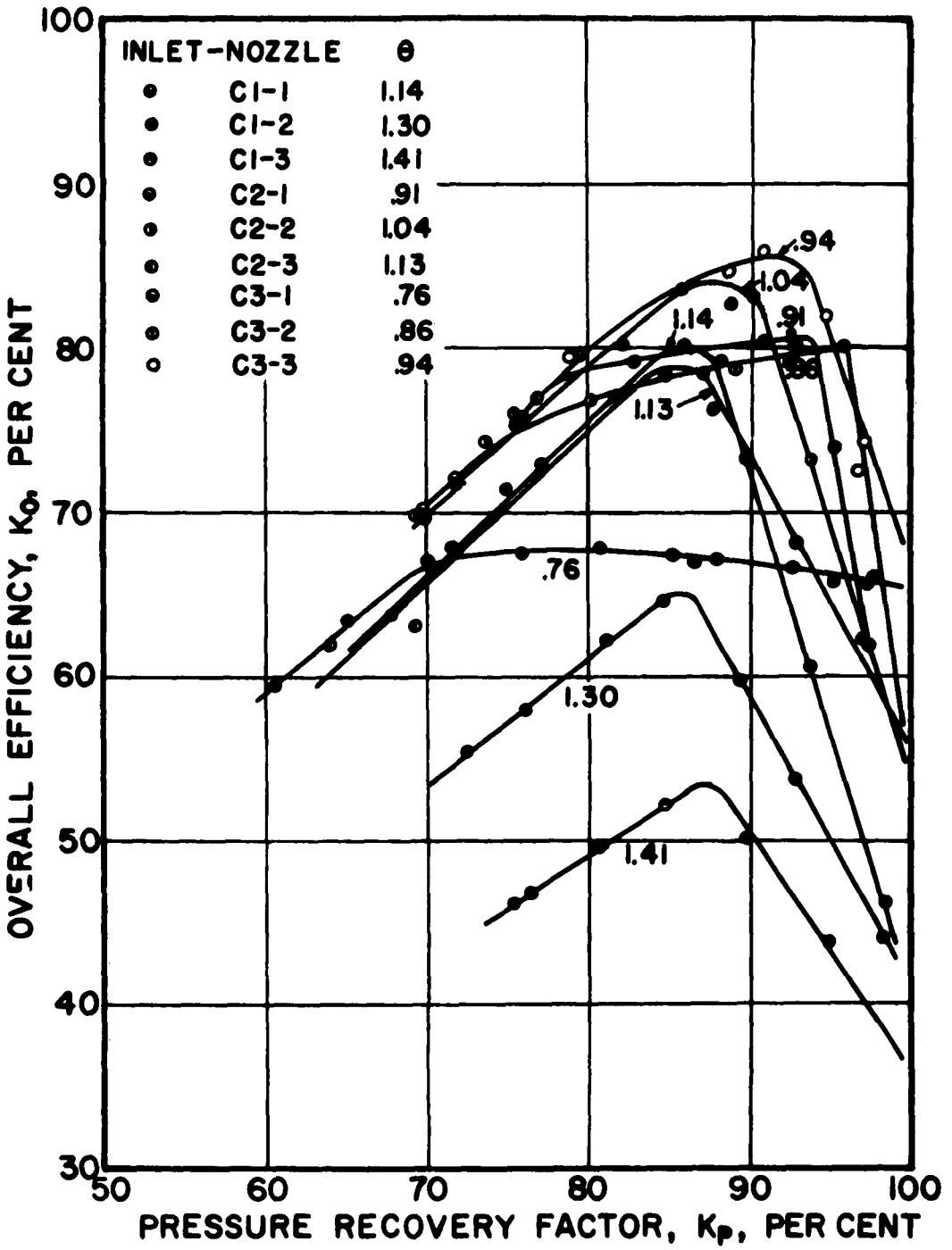

Fig. 7 Overall Efficiency as a Function of the Pressure Recovery Factor for Nozzles 1, 2, and 3 and Converging-Diverging Inlets C1, C2, and C3

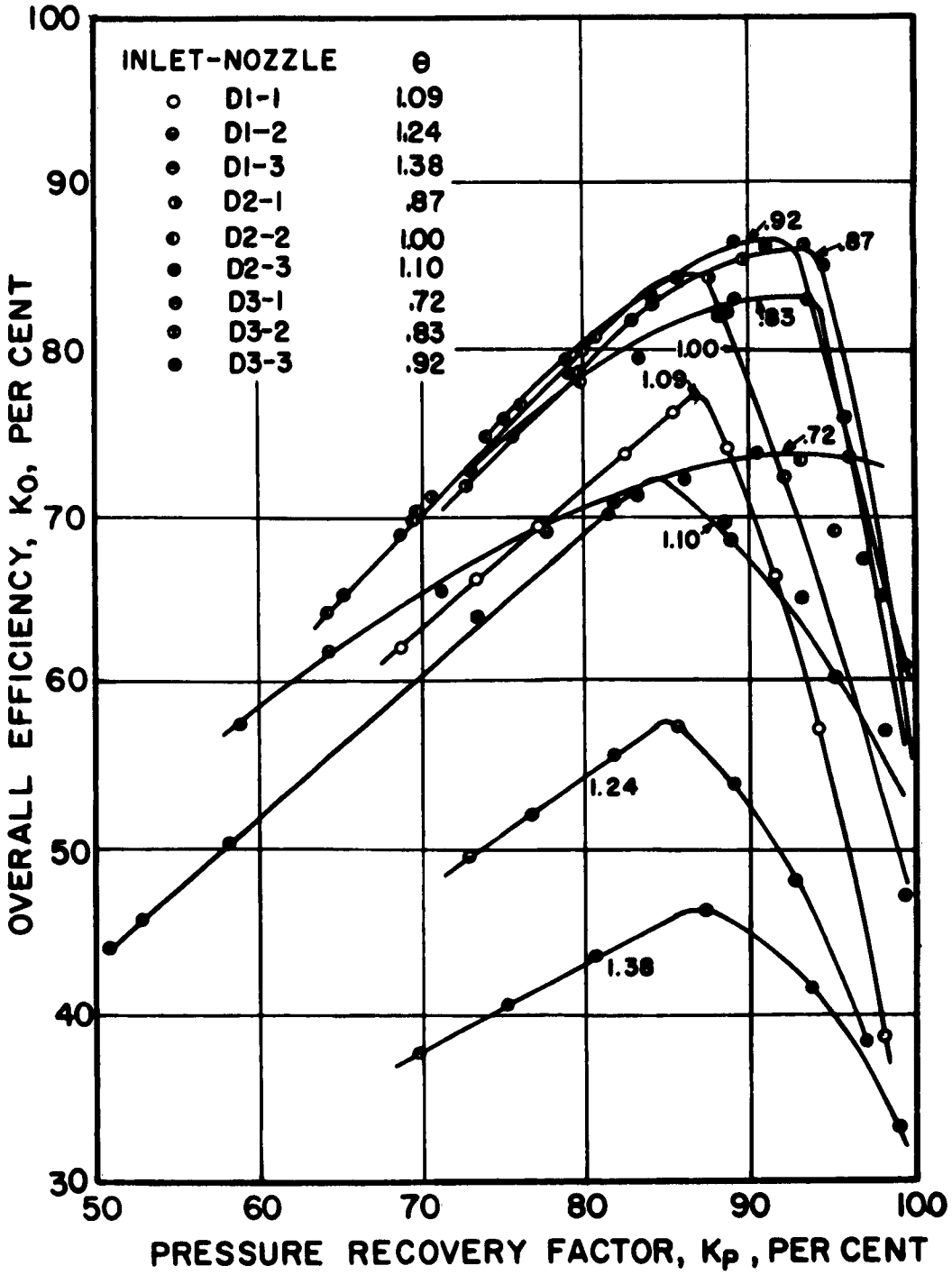

Fig. 8 Overall Efficiency as a Function of the Pressure Recovery Factor for Nozzles 1, 2, and 3 and Diverging Inlets D1, D2, and D3

Table 3

Values of the Jet-Inlet Diameter Ratio θ
for the Series II Free-Jet Experiments

(a) Converging-Diverging Inlets

Nozzle	Inlet C1	Inlet C2	Inlet C3
1	1.14	0.91	0.76
2	1.30	1.04	0.86
3	1.41	1.13	0.94

(b) Diverging Inlets

Nozzle	Inlet D1	Inlet D2	Inlet D3
1	1.09	0.87	0.72
2	1.24	1.00	0.83
3	1.38	1.10	0.92

Figure 9 presents $(K_0)_{MAX}$ as a function of θ for diffusers with converging-diverging inlets, and with diverging inlets. The curves present the peak values of K_0 obtained, denoted by $(K_0)_{MAX}$, for each value of θ investigated.

3-4 Gas Entrainment Experiments

Figure 10 illustrates schematically the apparatus employed for conducting the gas entrainment experiments. Since a detailed description of that apparatus is presented in Reference 11, only a brief description is presented here.

All of the gas entrainment experiments were conducted under connected-pipe conditions of entrance. An air injector located in the

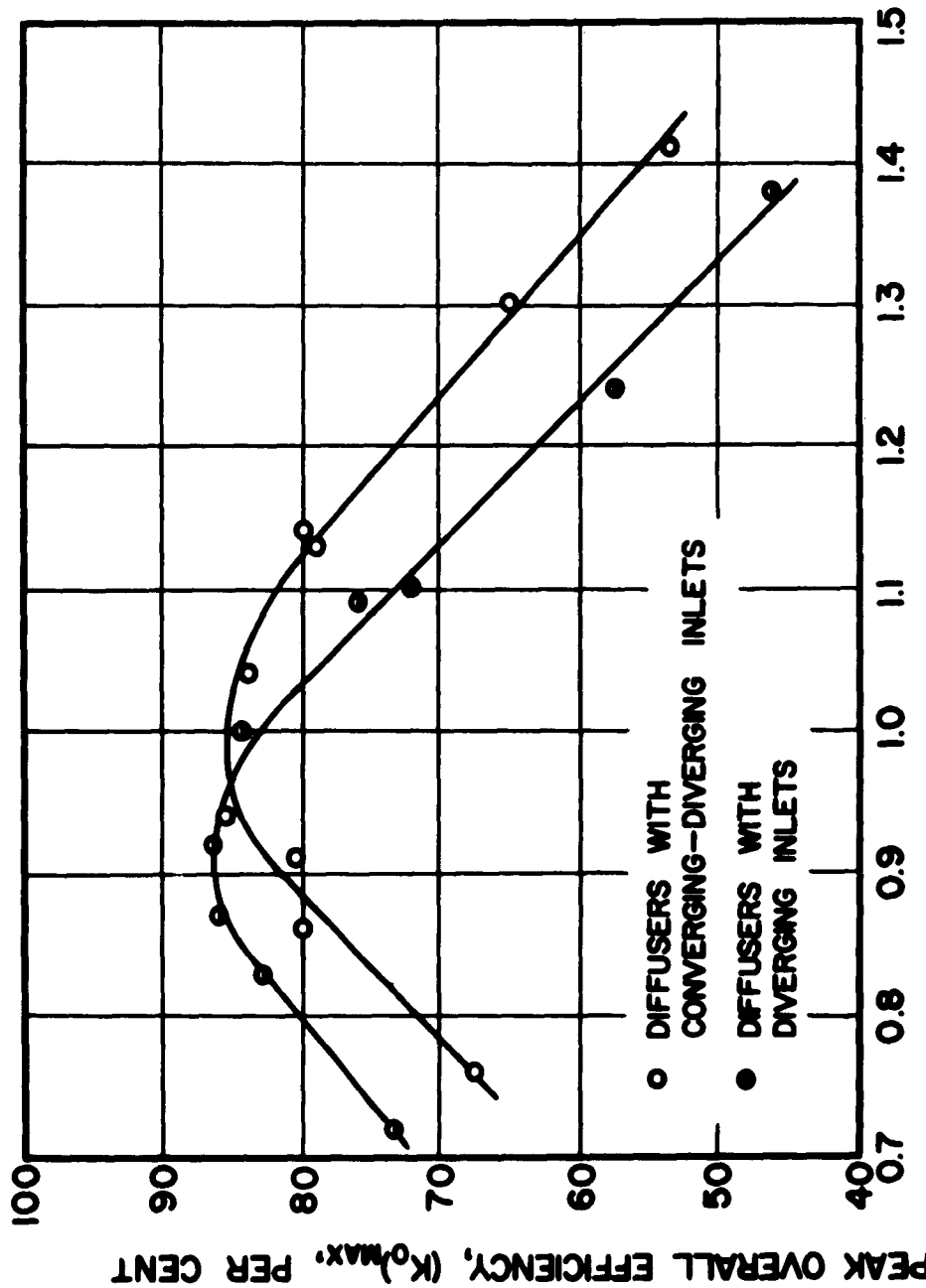

Fig. 9 Peak Overall Efficiency as a Function of the Jet-Inlet Diameter Ratio

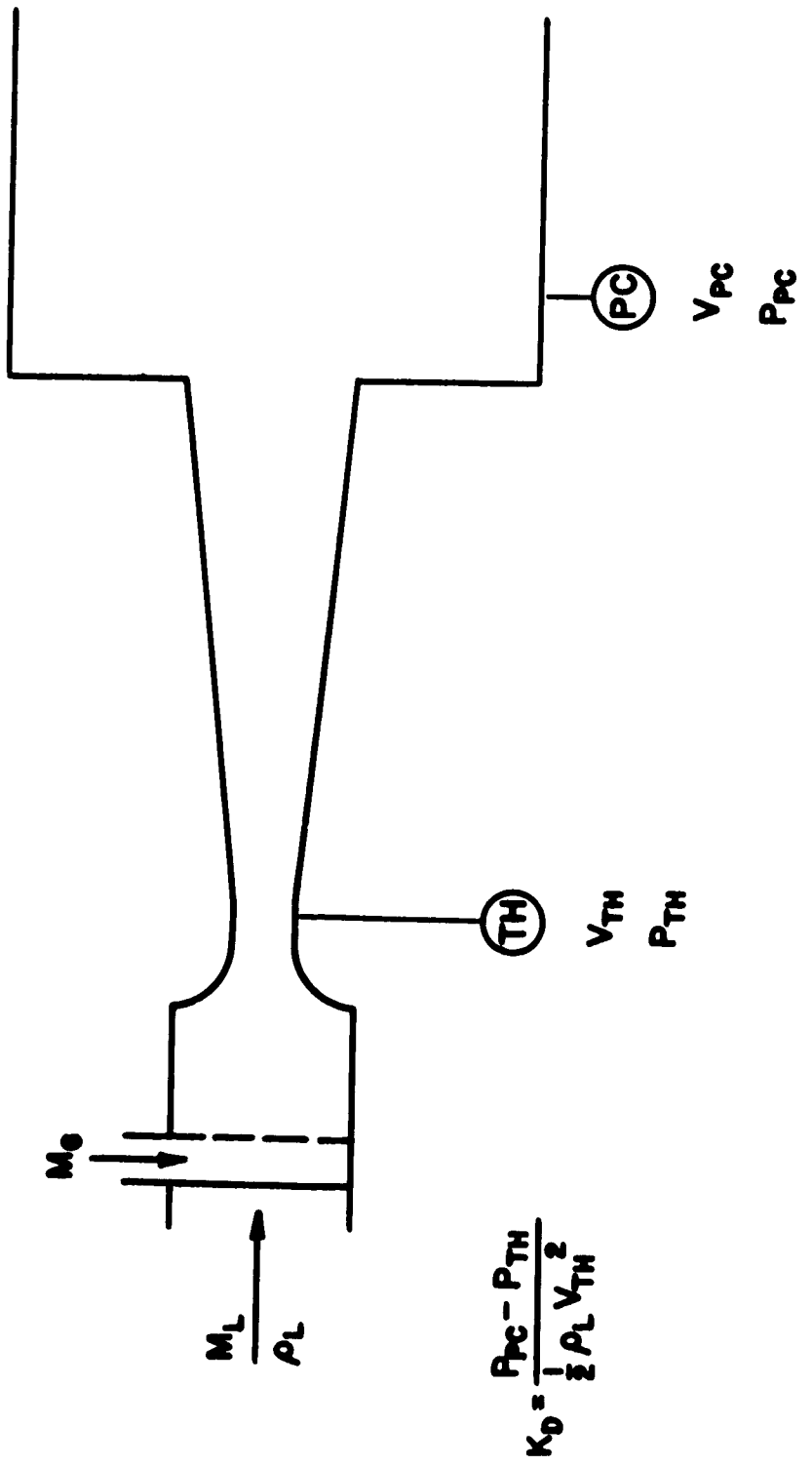

Fig. 10 Schematic Diagram of the Gas Entrainment Experimental Apparatus

water line upstream from the diffuser, provided a means for supplying a two-phase mixture of air and water to the diffuser. By adjusting the control valves in the air and water supply lines upstream from the air injector, the air and water flow rates could be varied. Figure 11 is a photograph of the experimental apparatus mounted on the test stand for the gas entrainment experiments.

The diffusing section was preceded by a rounded, converging nozzle, so that the velocity at the inlet to the diffuser was approximately uniform across the stream. The diameter of the conical diffusing section increased from 0.400 in. at the throat to 1.200 in. at the exit section; the total angle of divergence was 7°. The diffuser discharged into a plenum chamber. A valve downstream from the plenum chamber was employed for controlling the back pressure, and hence the static pressure at the throat of the diffuser, denoted by P_{TH}.

The pressure recovery parameter employed for these experiments is the diffuser efficiency, defined by

$$K_D = (P_{PC} - P_{TH}) / \tfrac{1}{2}\rho_L V_{TH}^2 \qquad (3\text{-}7)$$

where P_{PC} and P_{TH} are the static pressures measured at the plenum chamber and the diffuser throat, respectively, ρ_L is the density of the liquid, and V_{TH} is the velocity of the two-phase mixture at the throat; the flow at the throat was assumed to be one-dimensional.

The volumetric gas entrainment in the mixture crossing the throat section is defined by

$$E = Q_G / (Q_G + Q_L) \qquad (3\text{-}8)$$

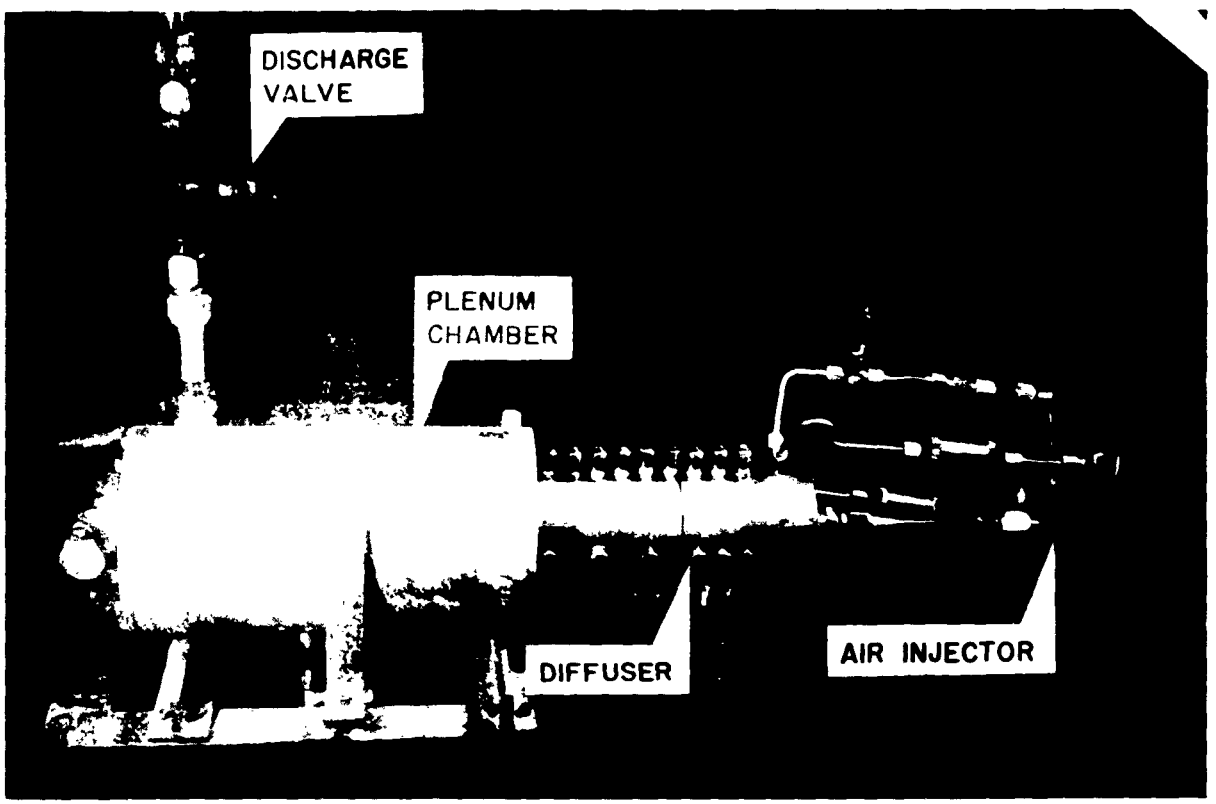

Fig. 11 Diffuser Apparatus Mounted on the Test Stand for the Gas Entrainment Experiments

where Q_G and Q_L are the volumetric rates of flow of the gas and the liquid, respectively, measured at the throat section of the diffuser.

Two methods for conducting the gas entrainment experiments were investigated. In the first method the mass rate of flow of the liquid M_L was held constant while the mass rate of flow of the gas M_G was varied. In the second method, both the gas and the liquid flow rates were varied in such a way that the velocity of the two-phase mixture at the throat of the diffuser V_{TH} was a constant. Since the second method permitted data points to be taken over a greater range of the values of the pertinent parameters, it was the method employed in the experiments to be discussed. In all of the experiments the throat velocity was V_{TH} = 95 fps, and the throat pressures investigated were P_{TH} = 30, 40, 50, and 60 psia.

Quantities measured and calculated for each data point were P_{PC}, P_{TH}, M_L, M_G, and the temperature of the two-phase mixture at the throat of the diffuser T_{TH}. From these data K_D was determined as a function of the volumetric gas entrainment E in the mixture crossing the throat section of the diffuser (see equation 3-8).

Figure 12 presents the diffuser efficiency K_D as a function of the volumetric gas entrainment E, with the throat pressure P_{TH} as a parameter.

The theoretical diffuser efficiency K_D for the isentropic flow of a two-phase mixture of a gas and a liquid, with no internal temperature difference, is approximately given by

$$K_D = 1 + \frac{M_G}{M_L}\left(1 - \frac{2R_G T_{TH}}{V_{TH}^2} \ln \frac{P_{PC}}{P_{TH}}\right) \qquad (3\text{-}9)$$

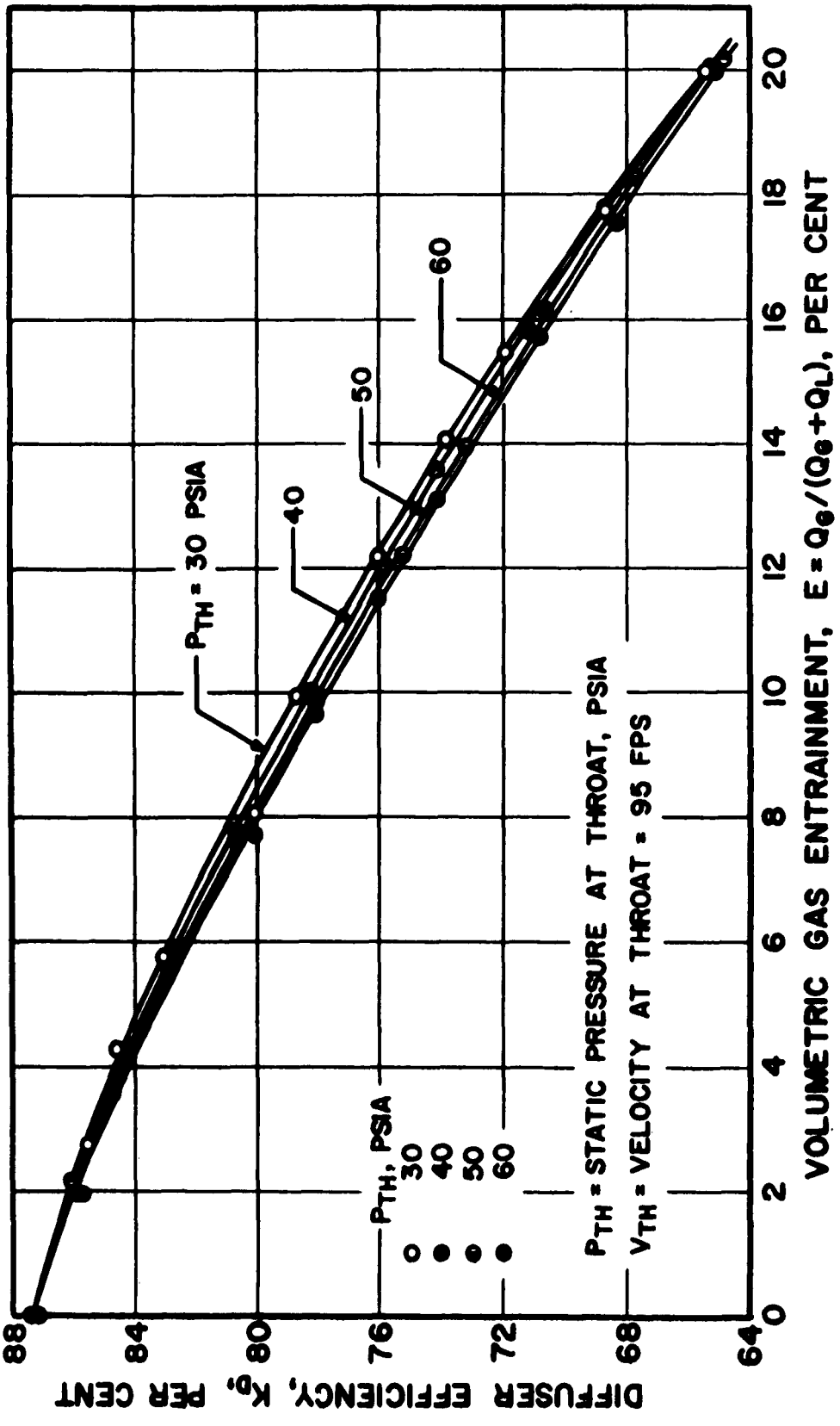

Fig. 12 Diffuser Efficiency as a Function of the Volumetric Gas Entrainment

The derivation of equation 3-9 is presented in Appendix D.

Figure 13 presents K_D (calculated by means of equation 3-9) as a function of the volumetric gas entrainment E for the two-phase flow of a mixture of water and air at throat pressures of P_{TH} = 30 and 60 psia and a throat velocity of V_{TH} = 95 fps. For comparison two of the experimental curves presented in Figure 12 are also plotted in Figure 13.

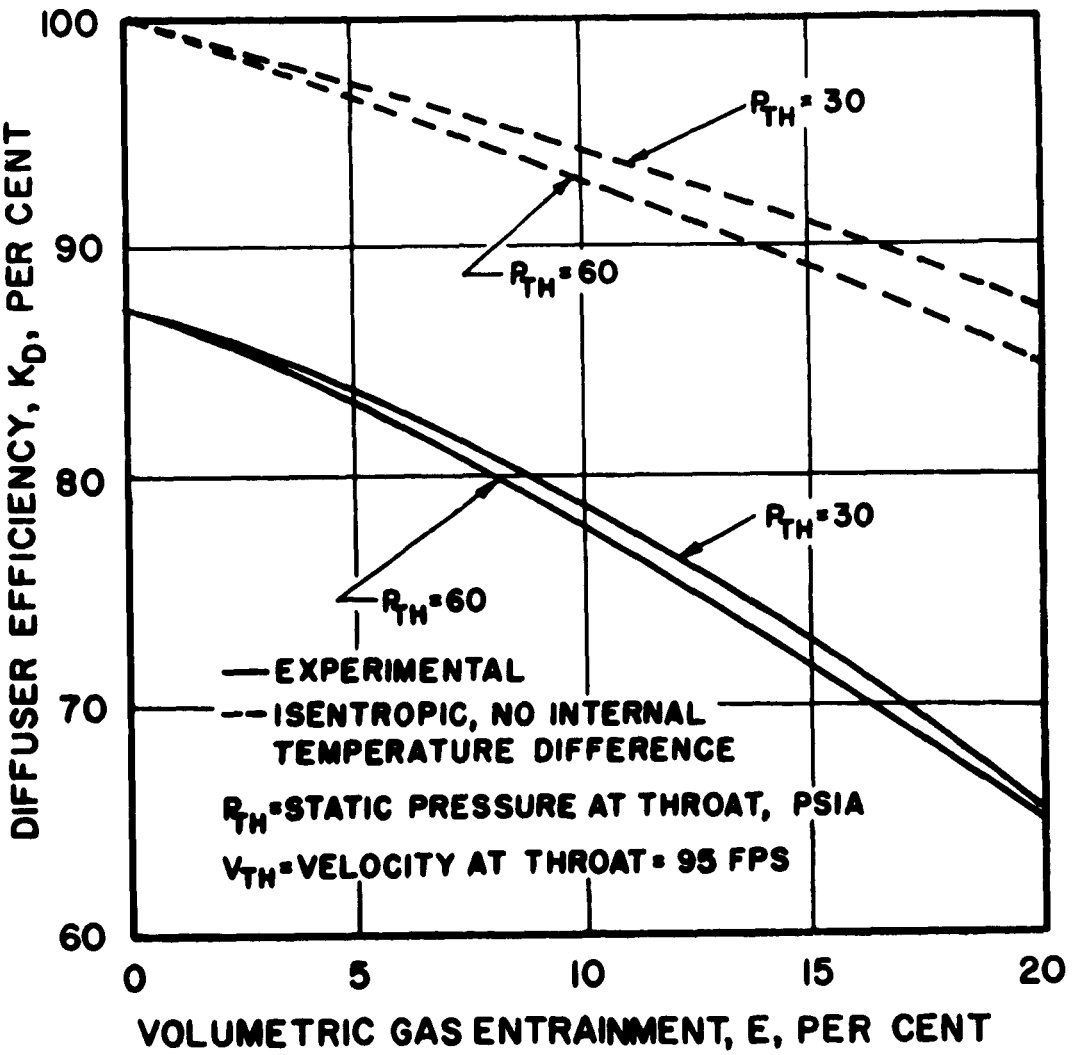

Fig. 13 Analytical and Experimental Two-Phase Diffuser Efficiencies

4 DISCUSSION OF THE EXPERIMENTAL RESULTS

4-1 Free-Jet Experiments

Since the discharge pressure in the Series I-a free-jet experiments was not controlled to give values of the pressure recovery factor K_P which could be readily compared for the various nozzle-inlet combinations employed, little information of practical importance was obtained from those experiments. It was observed, however, that the nozzle-inlet distance L and the liquid flow rate M_L had little effect on the performance characteristics of the diffuser. It is hypothesized that variations in L and M_L affected the diffuser performance only insofar as they (1) changed the diameter of the free jet entering the diffuser, or (2) caused gas to become entrained in the jet entering the diffuser. The hypothesis cannot be justified without additional experiments conducted so that the back pressure is controlled and the gas entrainment is measured.

Although the back pressure was varied in the Series I-b free-jet experiments, the nozzles and inlets employed did not give a large enough range of values for the jet-inlet diameter ratio θ, to yield significant results regarding the influence of θ.

The Series II free-jet experiments indicated that each nozzle-inlet combination, when investigated with a constant flow rate M_L and

a constant nozzle-inlet distance L, had a pressure recovery factor K_P for which the overall efficiency K_O was a maximum (see Figures 7 and 8). For the nozzle-inlet combinations employed, this value of K_P was between 79 and 96 per cent, and the corresponding values of $(K_O)_{MAX}$ ranged from 46 to 86.5 per cent.

It is of interest to examine the relative magnitudes of K_P and K_{CAP} under conditions yielding high values of K_O. Table 4 presents some experimental data points for which K_O was greater than 80 per cent. It is apparent that the highest values of K_O occur when K_P and K_{CAP} are of the order of 90 and 95 per cent, respectively.

The curves obtained by plotting K_O as a function of K_D for a given nozzle-inlet combination (Figures 7 and 8) peak sharply for values of jet-inlet diameter ratio θ larger than unity. As θ is decreased, however, the top of the curves flatten out. The flattening is ascribed to the behavior of the jets for smaller values of θ; they showed a smaller tendency to "spill over" the outside of the diffuser inlet. The jets for smaller values of θ gave low values of energy recovery, due probably to separation of the flow from the walls of the diffuser; a jet for a small θ does not fill the flow channel when it enters the diffuser.

The Series II free-jet experiments also indicated that there was, for each type of inlet investigated, a jet-inlet diameter ratio θ for which $(K_O)_{MAX}$ (the peak value of K_O for a given θ) had a maximum value. Figure 9 shows that for the converging-diverging inlet, the largest value of $(K_O)_{MAX}$ occurs at a jet-inlet diameter ratio of

Table 4

Sample Data for the Free-Jet Experiments

(a) Converging-Diverging Inlets

Inlet	Nozzle	θ	K_P	K_{CAP}	K_O
C2	2	1.04	85.7	97.5	83.6
C3	3	0.94	88.6	95.5	84.6
C3	3	0.94	90.9	94.4	85.8
C3	3	0.94	94.7	86.7	82.1

(b) Diverging Inlets

Inlet	Nozzle	θ	K_P	K_{CAP}	K_O
D3	3	0.92	89.2	97.1	86.6
D3	3	0.92	91.2	94.8	86.5
D2	1	0.87	93.5	92.4	86.4
D2	1	0.87	94.6	89.9	85.1

$\theta = 0.99$. The corresponding value of the peak overall efficiency is $(K_O)_{MAX} = 86$ per cent. For the diverging inlet the largest value of $(K_O)_{MAX}$ was 86.5 per cent and occurred at $\theta = 0.91$.

From Figure 9, it appears that for applications where θ may at times exceed unity, it would be desirable to employ a converging-diverging inlet, since the latter type of inlet yields higher energy recoveries for θ larger than unity. The afore-mentioned conclusion is also intuitively obvious, since the converging-diverging inlet provides a means for "funneling" a jet, having a diameter larger than

the throat diameter of the diffuser, into the diffuser.

It is not obvious, however, that the diverging inlet would give better energy recovery than the converging-diverging inlet for values of jet-inlet diameter ratio θ less than approximately unity, as is shown in Figure 9. In fact, one would expect the two types of inlets to yield the same values of $(K_O)_{MAX}$ when θ is less than unity.

Accurate measurements of the amount of gas entering the diffuser could not be made when the free-jet experiments were performed. There is reason to believe that gas entrainment was responsible for a portion of the energy losses in the diffuser, particularly when the free jet was considerably smaller than the diffuser inlet throat diameter.

4-2 Gas Entrainment Experiments

The results of the gas entrainment experiments agree qualitatively with the diffuser efficiency curves obtained assuming isentropic two-phase flow with no internal temperature difference. In both the experimental and the analytical results the diffuser efficiency K_D decreases with an increase in volumetric air entrainment E. Also, for a given value of E, K_D decreases when the static pressure at the throat of the diffuser P_{TH} increases.

As can be seen from Figure 13, however, for given values of E and throat pressure P_{TH} there is a large difference in the values of diffuser efficiency K_D obtained from the experiment and the predicted values based on analysis; the experimental values of K_D were much smaller than the predicted values. One may explain the disagreement between experiment and theory on the basis discussed below.

There are three types of energy losses associated with a two-phase mixture flowing through a diffuser. First, is the work required to compress the entrained gas, and that type of loss was the only one accounted for in the theoretical analysis. Second, there is the inherent diffuser loss, which occurs even when liquid alone is flowing through the diffuser; for the diffuser employed in these experiments, this loss, which is caused by friction and turbulent energy dissipation, is approximately 12.7 per cent of the entering kinetic energy. Third, there is an additional loss, which will be called the "two-phase" loss and denoted as L_{TP}, which occurs because a diffuser does not diffuse a two-phase fluid as efficiently as a single fluid, even when the compression work is not considered.

Table 5 presents the values of these three losses for throat pressures of P_{TH} = 30 and 60 psia, and volumetric gas entrainments of E = 0, 5, 10, 15, and 20 per cent.

It should be noted that the two-phase loss is not due to increased pressure drop in the direction of flow because of wall friction, since it may be shown by the method of Chenoweth and Martin (1) that for a constant throat velocity the pressure drop due to wall friction is smaller for a two-phase flow than for a single-phase liquid flow.

Since the two-phase loss is appreciably smaller than the other two losses for values of volumetric gas entrainment less than 5 per cent, the theoretical curve gives a fair approximation (within 25 per cent) of the decrease in diffuser efficiency to be expected with

Table 5

Energy Loss Analysis for the Gas Entrainment Experiments

(a) P_{TH} = 30 psia	Volumetric Gas Entrainment, per cent E = 0	5	10	15	20
Diffuser Efficiency, K_D	87.3	83.8	78.7	72.6	65.4
Inherent Loss	12.7	12.7	12.7	12.7	12.7
Compression Loss	0	2.8	5.9	9.1	12.6
Two-Phase Loss, L_{TP}	0	0.7	2.7	5.6	9.3

(b) P_{TH} = 60 psia	Volumetric Gas Entrainment, per cent E = 0	5	10	15	20
Diffuser Efficiency, K_D	87.3	83.2	77.7	71.7	65.0
Inherent Loss	12.7	12.7	12.7	12.7	12.7
Compression Loss	0	3.5	7.2	11.1	15.2
Two-Phase Loss, L_{TP}	0	0.6	2.4	4.5	7.1

two-phase flow. Therefore, if the inherent, single fluid loss is known, the total loss may be approximated for values of volumetric gas entrainment up to 5 per cent, if the throat velocity is approximately 95 fps. For values of volumetric gas entrainment greater than 5 per cent, however, the total loss in efficiency will be considerably larger than the combined compression and inherent losses.

In actual jet pump applications, the throat velocity would be several times that investigated in these experiments. Figure 14 presents the diffuser efficiency K_D as a function of the volumetric gas entrainment E for the isentropic, no internal temperature

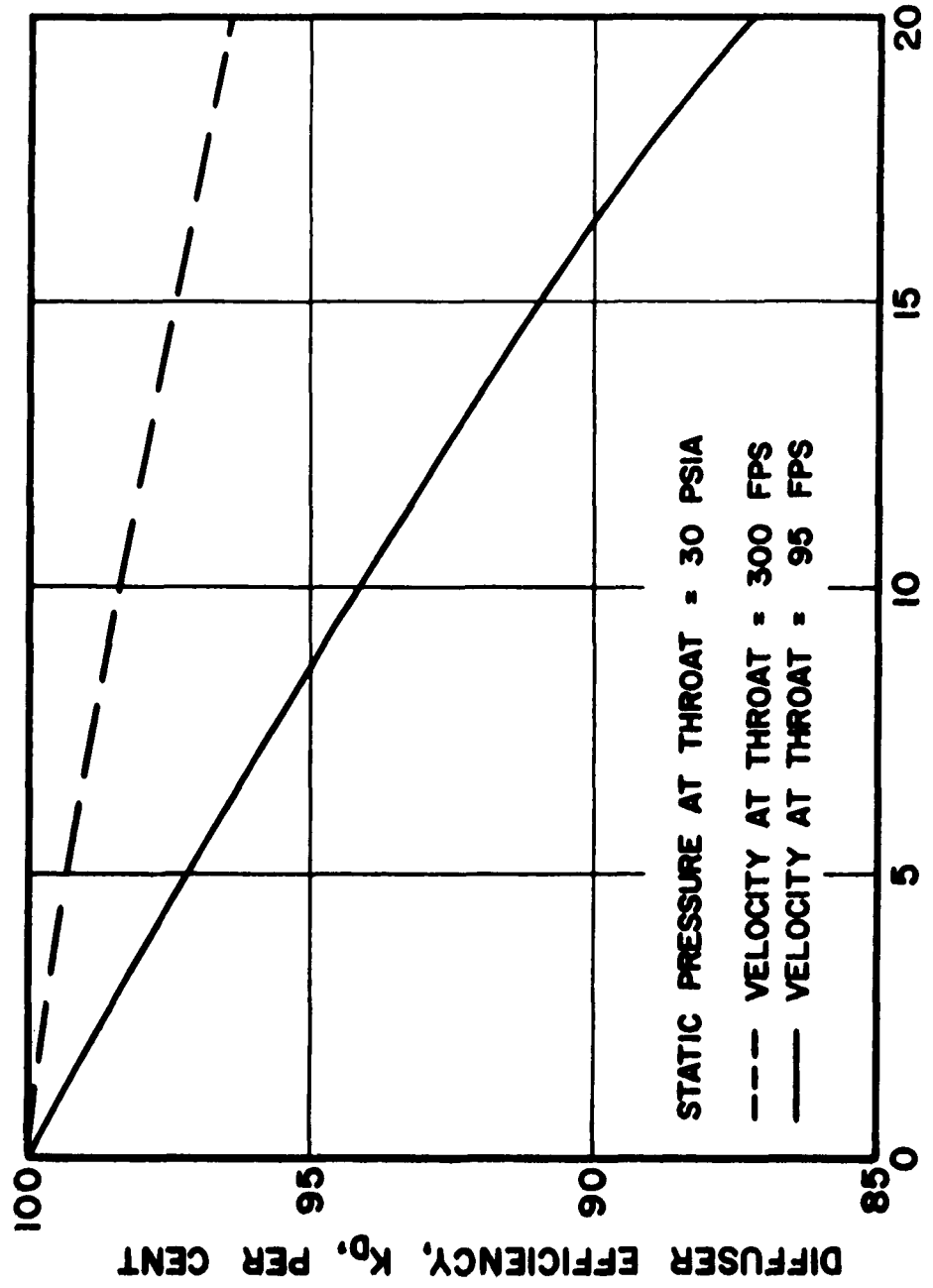

Fig. 14 Effect of the Throat Velocity on the Diffuser Efficiency for Two-Phase Isentropic Flow

difference flow of air and water with a throat pressure of P_{TH} = 30 psia. Throat velocities of V_{TH} = 95 and 300 fps are shown. It is apparent that the decrease in K_D for isentropic flow is less for diffusers with high throat velocities than for those with lower throat velocities. Preliminary experiments showed that for the flow of only water, the velocity had little effect on the inherent diffuser loss. Therefore, assuming that the two-phase loss does not increase when the throat velocity increases, it follows that, for a given volumetric gas entrainment E, the diffuser efficiency K_D of a two-phase diffuser increases as the throat velocity increases.

The experimental results of Karplus (5), which came to the attention of the present investigator only after the research reported herein had been completed, may have considerable bearing on the results of the gas entrainment experiments.

Karplus found that the acoustic velocity of a two-phase mixture of air and water may be very much lower than that of water alone. Since his experiments show that the acoustic velocity of an air-water mixture is 95 fps for a volumetric air entrainment of E = 12 per cent, it would follow that with that air entrainment, the Mach number, defined as the local velocity of the fluid divided by the local acoustic velocity, at the throat of the diffuser during the gas entrainment experiments would equal one. And at values of E greater than 12 per cent, the flow at the throat would be supersonic, i.e., the throat velocity would be greater than the local sonic velocity. The exact effect such a condition would have on the diffuser

performance is unknown, due to the limited knowledge of this type of two-phase flow.

It was of interest, however, to attempt a correlation of the results of the gas entrainment experiments, basing the correlation on the Mach number at the throat of the diffuser, denoted as M_{TH}. This was accomplished in the following manner, with full realization that the results of the correlation may have little or no validity, because of the limited knowledge regarding the characteristics of the two-phase flow, and also the simplicity of the method of correlation.

It was assumed that the two-phase loss, denoted L_{TP}, was a function only of the Mach number at the throat of the diffuser, M_{TH}, such that

$$L_{TP} = A\ (M_{TH})^{B} \qquad (4\text{-}1)$$

The constants A and B in equation 4-1 were evaluated for both throat pressures of 30 and 60 psia, based on the values of the two-phase loss appearing in Table 5. The correlation was made to agree exactly with the experimental values of the two-phase losses corresponding to E = 0, 10, and 20 per cent. The results of that correlation are

$$P_{TH} = 30 \text{ psia:}\quad L_{TP} = 2.9\ (M_{TH})^{4.5}$$

$$P_{TH} = 60 \text{ psia:}\quad L_{TP} = 2.2\ (M_{TH})^{4.0}$$

Based on the foregoing correlation, the two-phase loss is strongly dependent on the Mach number at the throat of the diffuser. Referring to the earlier discussion of the effect that increasing the throat velocity would have on the diffuser efficiency, it is seen that

although the compression loss may be smaller for a higher throat velocity than for that investigated, the two-phase loss may become extremely large at a higher velocity, even for fairly moderate values of air entrainment. For example, if P_{TH} = 60 psia, V_{TH} = 300 fps, and E = 5 per cent, then, according to Karplus, M_{TH} = 2.24 and hence, employing the correlation just developed, L_{TP} = 55 per cent!

It is admitted that the latter result was obtained by an argument based on limited information. Nevertheless, it points out the possible importance of compressibility effects in two-phase diffuser flow.

5 CONCLUSIONS AND RECOMMENDATIONS

5-1 Conclusions

1. It is possible to design a diffuser inlet which will enable 86.5 per cent of the kinetic energy of a free jet of liquid to be recovered in the diffuser. (In a free-jet experiment 95.1 per cent of the jet was captured by the diffuser and 91 per cent of the kinetic energy of the captured jet was converted to static pressure.)

2. For maximum total energy recovery, the jet-inlet diameter ratio should be 0.91 for a diffuser with a diverging inlet and 0.99 for a diffuser with a converging-diverging inlet.

3. Entrained gas in a free jet entering a diffuser is detrimental to the pressure recovery characteristics of the diffuser.

4. For values of volumetric gas entrainment less than 5 per cent and a throat velocity of 95 fps, the decrease in diffuser efficiency caused by the entrained gas is approximately the same for an actual diffuser flow as for isentropic flow with no internal temperature difference. For values of volumetric gas entrainment greater than 5 per cent, the energy loss will be significantly larger than that for the isentropic flow.

5. The relatively low sonic velocities encountered in two-phase diffuser flow are a possible source of compressibility effects which may seriously reduce the energy recovery in the diffuser.

5-2 Recommendations

1. Additional investigation of the effects that entrained gas has on the diffusion of a liquid are required, since the results reported herein indicate that gas entrainment may greatly decrease the pressure recovery of the diffuser. In particular, this problem must be investigated with velocities considerably higher than those corresponding to Mach 1 at the inlet of the diffuser.

2. Following additional gas entrainment experiments, free-jet experiments conducted with a two-phase jet rather than a liquid jet should be conducted to obtain information on the characteristics of two-phase diffusion flow with free-jet entrance conditions. Such experiments will no doubt be more difficult to perform, because of the increased number of variables. Also, it is expected that additional "side" problems, such as the divergence of the jet, would be encountered. Such experiments are needed, however, because of the lack of information on the characteristics of two-phase flows.

LIST OF REFERENCES

1. Chenoweth, J. M. and Martin, M. W., "Pressure Drop of Gas-Liquid Mixtures in Horizontal Pipes," Petroleum Engineering, vol. 28, no. 4, April 1956.

2. Crabtree, D. L., "Investigation of the Influence of the Design Parameters on the Flow Characteristics of the Drive Nozzle of a Gas-Driven Jet Pump," M.S.M.E. Thesis, Purdue University, Lafayette, Indiana, 1961.

3. Elliott, D. G., "Theoretical and Experimental Investigation of a Gas-Driven Jet Pump for Rocket Engines," Ph.D. Thesis, Purdue University, Lafayette, Indiana, 1959. (Classified) (The declassified portions of the afore-mentioned reference as employed herein appear in Liquid Rockets and Propellants, Progress in Astronautics and Rocketry, vol. 2, Academic Press, New York, 1960.)

4. Gibson, A. H., "On the Resistance to Flow of Water Through Pipes or Passages having Divergent Boundaries," Trans. Royal Society of Edinburgh, vol. 48, part 1, 1913.

5. Karplus, "The Velocity of Sound in a Liquid Containing Gas Bubbles," AEC Research and Development Report, COO-248, Contract No. AF(11-1)-528, Armour Research Foundation, Illinois Institute of Technology, Chicago, Illinois.

6. Kline, S. J., Abbott, D. E., and Fox, R. W., "Optimum Design of Straight-Walled Diffusers," Journal of Basic Engineering, Transactions of the ASME, September, 1959.

7. "Measurement of Quantity of Materials," Power Test Codes, Part 5, American Society of Mechanical Engineers, New York, 1959.

8. Patterson, G. N., "Modern Diffuser Design," Aircraft Engineering, vol. 10, September 1938, pp. 267-273.

9. Peters, H., "Conversion of Energy in Cross-Sectional Divergences Under Different Conditions of Inflow," NACA TM No. 737, March 1934.

10. Robertson, J. M., and Ross, D., "Effect of Entrance Conditions on Diffuser Flow," ASCE Proceedings, vol. 78, July 1952.

11. Schneiter, G. R., "Pressure Recovery for Single- and Two-Phase Flow through a Conical Diffuser with (a) Connected-Pipe and (b) Free-Jet Entrance Conditions," M.S.M.E. Thesis, Purdue University, Lafayette, Indiana, 1962.

APPENDICES

APPENDIX A

NOMENCLATURE

A	cross-sectional area of the free jet, ft^2.
A_{NOZ}	cross-sectional area of the nozzle exit, ft^2.
C_L	specific heat of the liquid, $B/lb_m R$.
C_P	constant pressure specific heat of the gas, $B/lb_m R$.
D_N	diameter of the nozzle exit, in.
D_{ST}	diameter of the free jet, measured at the plane of the throat of the diffuser, in.
D_{TH}	diameter of the throat of the diffuser, in.
E	volumetric gas entrainment, $Q_G / (Q_G + Q_L)$, per cent.
h	specific enthalpy, B/lb_m.
k	specific heat ratio of the gas.
K_{CAP}	capture efficiency, M_{CAP}/M_L, per cent.
K_D	diffuser efficiency, $(P_{PC} - P_{TH}) / \frac{1}{2}\rho_L V_{TH}^2$, per cent.
K_O	overall efficiency, $K_{CAP} K_P$, per cent.
$(K_O)_{MAX}$	peak value of the overall efficiency for a given value of the jet-inlet diameter ratio θ, per cent.
K_P	pressure recovery factor, $P_{PC} / \overline{P_{DYN}}$, per cent.
L	distance between the exit plane of the nozzle and the inlet plane of the diffuser, in.

L_{TH} distance between the exit plane of the nozzle and the plane of the throat of the diffuser, in.

L_{TP} "two-phase" energy loss in a two-phase diffuser, per cent.

M_{CAP} mass rate of flow of the liquid captured by the diffuser, lb_m/sec.

M_G mass rate of flow of the gas, lb_m/sec.

M_L mass rate of flow of the liquid, lb_m/sec.

M_{TH} Mach number at the throat of the diffuser.

p power in the power law relationship.

P pressure of the two-phase mixture, psfa.

P_{DYN} dynamic pressure at a point in a plane perpendicular to the axis of the free jet, psi.

P_{DYN}' nominal dynamic pressure of the free jet, $\frac{1}{2}\rho_L \bar{V}^2$, psi.

$\overline{P_{DYN}}$ mean dynamic pressure of the free jet, psi.

P_{PC} static pressure in the plenum chamber of the diffuser, or back pressure; psig (free-jet experiments), psia (gas entrainment experiments).

P_{TH} static pressure at the throat of the diffuser, psia.

ΔP_G differential pressure measured across the air orifice meter, psi.

ΔP_L differential pressure measured across the water orifice meter, psi.

Q_G volume rate of flow of the gas, measured at the throat of the diffuser, ft^3/sec.

Q_L volume rate of flow of the liquid, ft^3/sec.

r	radial distance from the center of the free jet, in.
R	radius of the free jet, in.
R_G	gas constant of the gas, ft-$lb_f/lb_m R$.
s	specific entropy, $B/lb_m R$.
Δs	change in the specific entropy between stations 1 and 2, $B/lb_m R$.
S	entropy of the two-phase mixture, B/R.
ΔS	change in the entropy of the two-phase mixture between stations 1 and 2, B/R.
T	temperature, R.
T_{TH}	temperature of the two-phase mixture at the throat of the diffuser, R.
u	specific internal energy, B/lb_m.
V	velocity, fps.
V_{TH}	mean velocity of the two-phase mixture at the throat of the diffuser, fps.
$\bar{V}$	mean velocity of the free jet, $M_L/\rho_L A_{NOZ}$, fps.
Y	expansion factor in the equation for the gas flow rate.
θ	ratio of the diameter of the free jet, measured at the plane of the throat of the diffuser (see Figure 1), to the diameter of the throat of the diffuser inlet, D_{ST}/D_{TH}.
ρ_G	density of the gas, lb_m/ft^3.
ρ_{GU}	density of the gas measured at the upstream tap of the air orifice meter, lb_m/ft^3.
ρ_L	density of the liquid, lb_m/ft^3.

ϕ ratio of the dynamic pressure to the nominal dynamic pressure of the free jet, P_{DYN}/P_{DYN}'.

ϕ_{MAX} maximum value of ϕ for a given nozzle.

Subscripts

1 throat of the diffuser (Appendix D).

2 plenum chamber (Appendix D).

G gas.

L liquid.

PC plenum chamber.

TH throat of the diffuser.

APPENDIX B

DETERMINATION OF THE DIAMETERS OF THE FREE JETS OF LIQUID FROM NOZZLES 1, 2, AND 3

B-1 Introduction

To correlate the data obtained from the free-jet experiments, one must know D_{TH} and D_{ST}, the diameters of the throat of the diffuser and of the free jet, respectively; the diameter D_{ST} is measured at the distance L_{TH} (see Figure 1) from the exit plane of the nozzle.

The throat diameter D_{TH} was measured with inside calipers and a micrometer. The determination of the jet diameter, however, was difficult for two reasons. First, the jet diverged after leaving the nozzle, so that the diameter of the jet was not equal to the exit diameter of the nozzle D_N. Second, the jet was surrounded by a fine spray, making it difficult to define the exact boundary of the jet.

In this appendix the photographic method employed for determining the diameters of the free jets of liquid downstream from Nozzles 1, 2, and 3 is presented.

B-2 Description of the Experimental Apparatus

Figure B-1 is a photograph of the apparatus employed for measuring the diameters of the free jets. A light, seen at the top of the photograph, was placed directly behind the free jet, relative to the

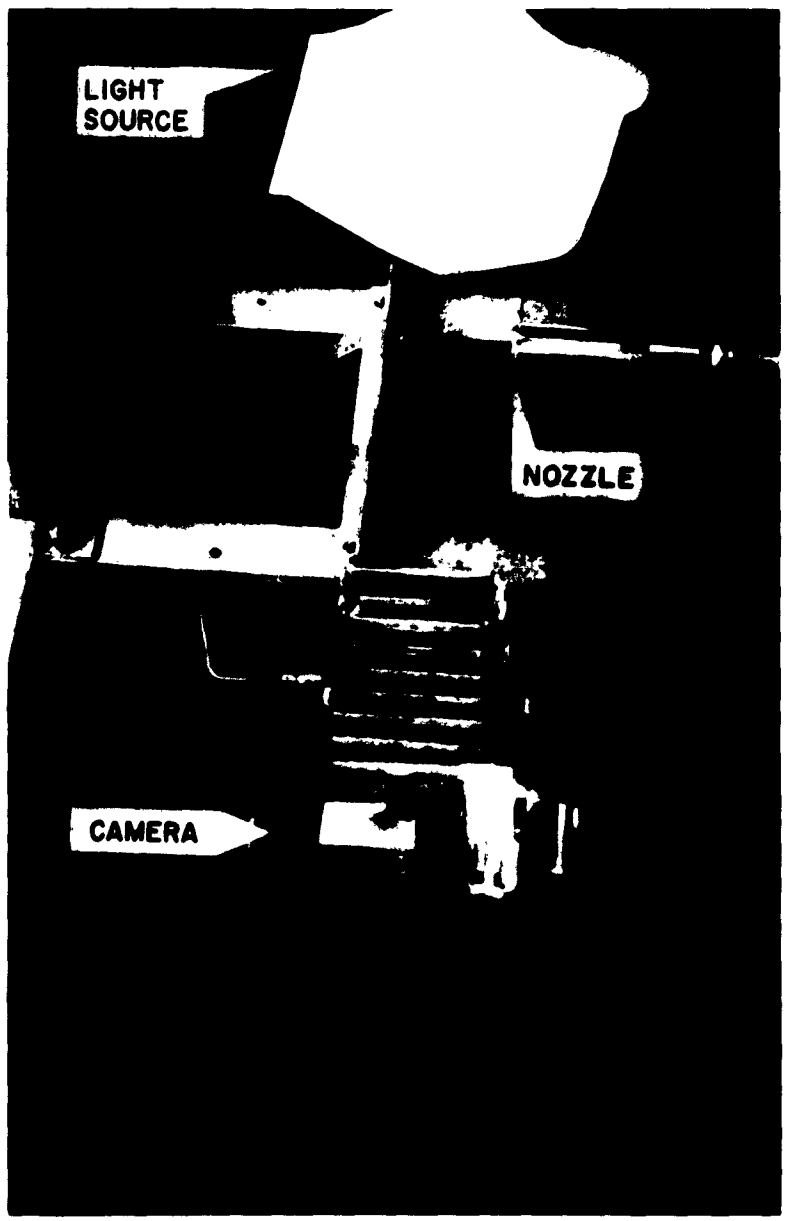

Fig. B-1 Apparatus for the Measurement of the Diameters of the Free Jets

camera. It was found with that arrangement the light penetrated the afore-mentioned spray, thus making the actual boundary of the jet more visible.

The light source was a No. 2 photoflood lamp in a reflector. A sheet of tracing paper was fastened over the reflector, but not in contact with the lamp, to diffuse the light from the source. The camera was a Crown Graphic 4 x 5 press camera mounted on a tripod. The axis of the nozzle and jet was parallel with the planes of the lens of the camera and the film. Consequently, the dimensions of the jet and nozzle were proportional to the respective dimensions of their images on the film.

B-3 Experimental Procedure

Photographs were taken of the jet from each nozzle at flow rates of M_L = 4, 6, 8, and 10 lb_m per sec. Exposures were 1/200 sec at f16 using Kodak Royal Pan film.

To facilitate the scaling of the image, an enlargement of each photograph was made on 8 x 10 in. glossy paper. Figure B-2 presents a smaller enlargement than that used for making the measurements.

The diameter of the nozzle exit was taken as the reference dimension, and all other dimensions were referred to it. Thus

$$\frac{\text{length on photograph}}{\text{actual length}} = \frac{\text{diameter of nozzle exit on photograph}}{\text{actual diameter of nozzle exit}}$$

The diameters of each jet were measured at positions 0.25, 0.50, 0.75, and 1.00 in. downstream from the nozzle.

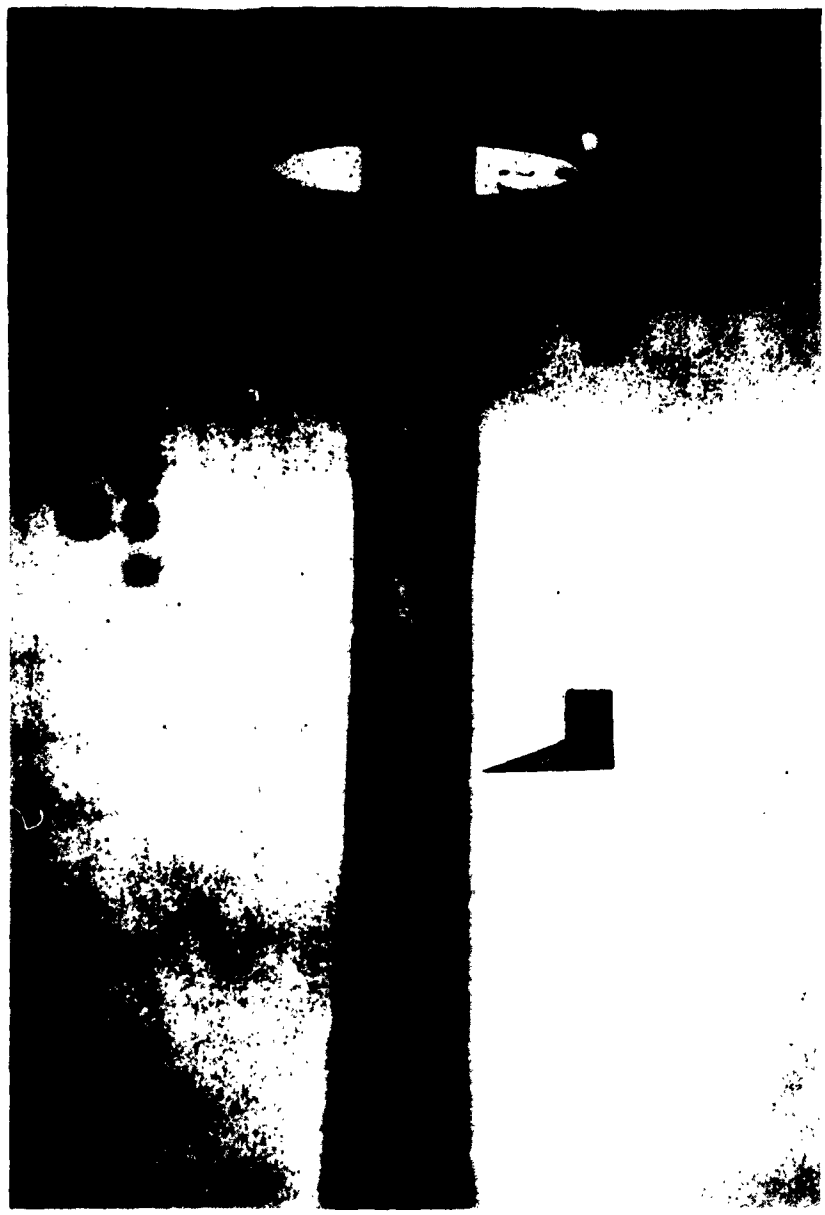

Fig. B-2 Sample Photograph of a Free Jet

B-4 Results

Figure B-3 presents the jet diameters as a function of the distance from the nozzle for Nozzles 1, 2, and 3, for a flow rate of M_L = 6 lb_m per sec (the value of M_L for the Series II free-jet experiments). A smooth curve was drawn through the data points for each nozzle, and the jet diameters employed in the Series II free-jet experiments were obtained from the smooth curves. Table B-1 presents the values of jet diameter obtained from such curves for Nozzles 1, 2, and 3, at distances of 0, 0.25, 0.50, 0.75, and 1.00 in. from the nozzle.

Table B-1

Jet Diameter as a Function of the Distance from the Nozzle for Nozzles 1, 2, and 3

	Distance from Nozzle, in.				
	0	0.25	0.50	0.75	1.00
Nozzle 1	0.350	0.362	0.371	0.378	0.384
Nozzle 2	0.402	0.414	0.423	0.431	0.437
Nozzle 3	0.452	0.459	0.465	0.470	0.474

B-5 Sources of Error

Possible sources of error in the experiments discussed herein, are discussed below.

a. The actual boundary of the jet may be different from that observed, due to refraction and reflection of light by the jet and the spray.

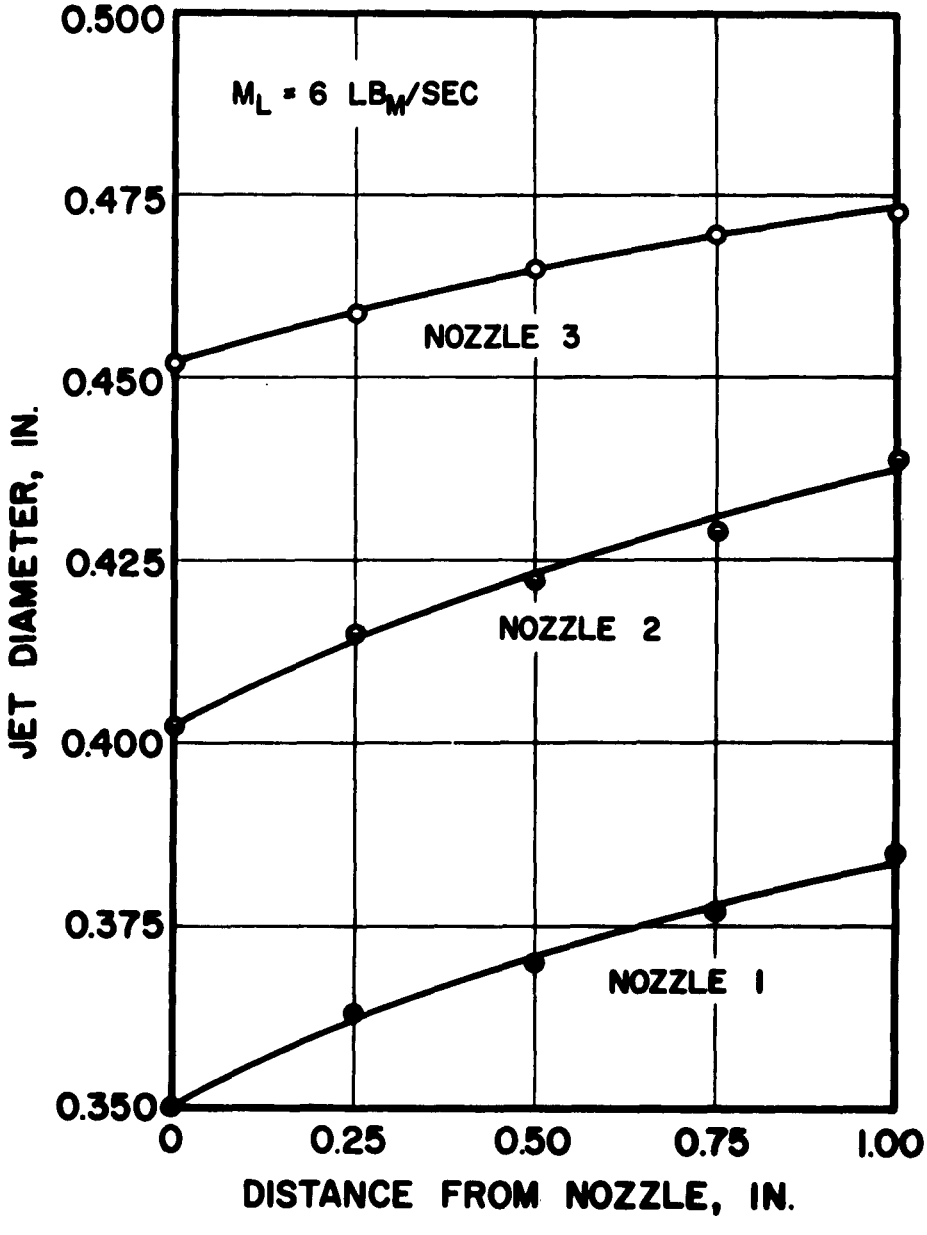

Fig. B-3 Diameter of the Free Jets as a Function of the Distance from the Nozzle for Nozzles 1, 2, and 3

b. Distortion of the photograph of the jet may be caused by improper alignment of the camera and the nozzle, and by improper alignment of the enlarger employed for making the 8 x 10 in. print.

c. The final image may be distorted due to stretching of the film and the photographic paper during processing.

d. Variations in the exposure and processing of the film and the photographic paper may cause some of the 8 x 10 in. prints to be lighter or darker than others. If that occurs, the photographed jet would appear either narrower or wider in such prints than if all the prints were exposed and processed in exactly the same manner.

e. Errors may be made in scaling the dimensions of the jet from the enlarged photographs.

APPENDIX C

DETERMINATION OF THE KINETIC ENERGIES OF THE FREE JETS OF LIQUID FROM NOZZLES 1, 2, AND 3

C-1 Introduction

The pressure recovery factor K_P is defined in the Series II free-jet experiments as

$$K_P = P_{PC} / \overline{P_{DYN}} \tag{C-1}$$

where $\overline{P_{DYN}}$ is the dynamic pressure representing the kinetic energy of the free jet. By definition

$$\overline{P_{DYN}} = \frac{1}{A}\int_A P_{DYN}\, dA \tag{C-2}$$

where A is the cross-sectional area of the jet at any given plane perpendicular to the axis of the jet, and

$$P_{DYN} = \frac{1}{2}\rho_L V^2 \tag{C-3}$$

is the dynamic pressure at any point in that plane. If it is assumed that the jet is of circular cross-section and that V, and hence P_{DYN}, is a function of the distance from the center of the jet only, equation C-2 may be written

$$\overline{P_{DYN}} = \frac{2}{R^2}\int_0^R r\, P_{DYN}\, dr \tag{C-4}$$

where R is the radius of the jet at the given plane, and r is the distance from the center of the jet.

It is necessary to know the relationship between P_{DYN} and r, so that $\overline{P_{DYN}}$ may be evaluated employing equation C-4. The method employed for determining the afore-mentioned relationship for Nozzles 1, 2, and 3 will now be described.

C-2 Description of the Experimental Apparatus

Figure C-1 is a photograph of the apparatus employed. A total pressure tube having an outside diameter of 0.020 in. and an inside diameter of 0.010 in. was mounted with its axis parallel with that of the nozzle. The tube was mounted at the vertex of a wedge having a total vertex angle of 20°. The wedge could be moved in the direction perpendicular to the axis of the nozzle. The end of the total pressure tube was between 0 and 0.01 in. downstream from the plane of the nozzle exit.

C-3 Experimental Procedure

The free jets from Nozzles 1, 2, and 3 were investigated at a flow rate of $M_L = 6\ lb_m$ per sec. For each jet, total pressure readings were taken every 0.018 in. along one diameter of the jet. Since the flow rate was not exactly the same for all of the data points, the ratio of the dynamic pressure P_{DYN} to a nominal dynamic pressure P_{DYN}' was calculated for each data point. This ratio is denoted by

$$\phi = P_{DYN}/P_{DYN}' \qquad (C\text{-}5)$$

The nominal dynamic pressure is defined as

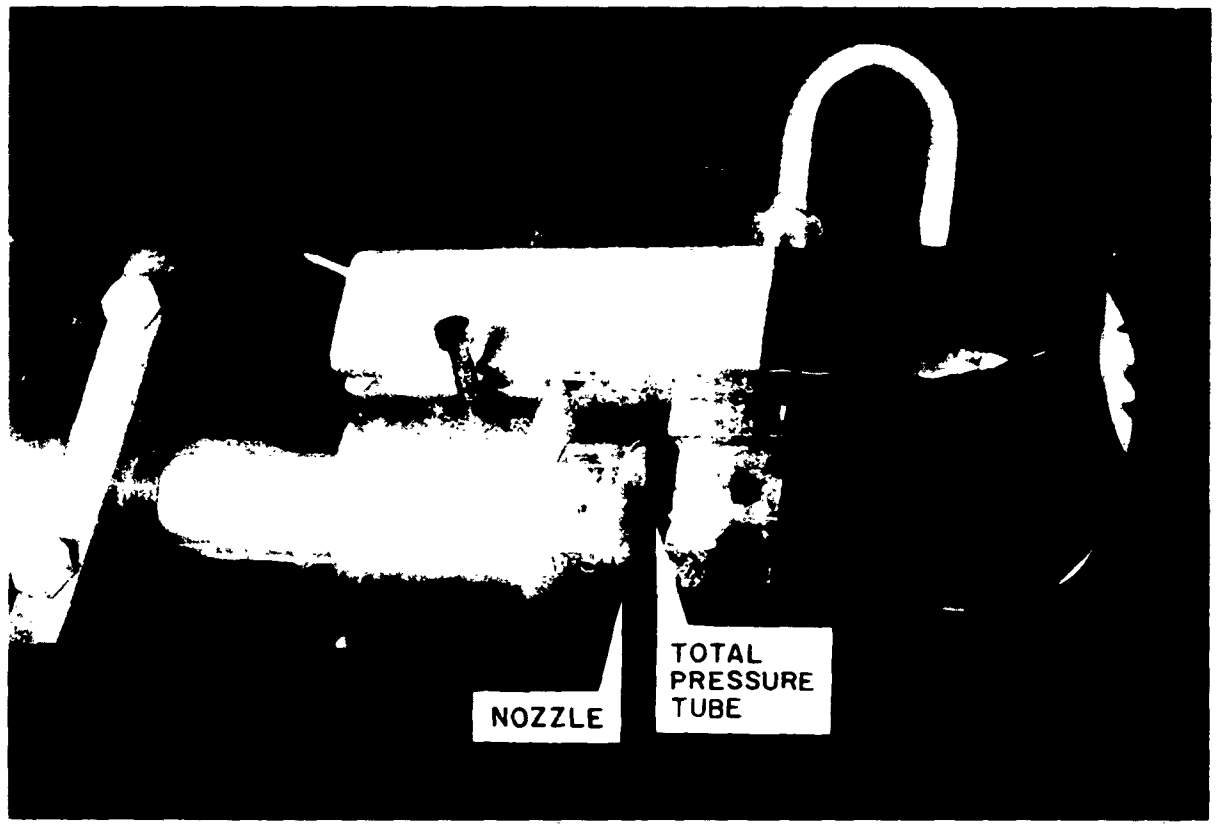

Fig. C-1 Apparatus for the Measurement of the Kinetic Energy of the Free Jets

$$P_{DYN}' = \frac{1}{2}\rho_L \bar{V}^2 \tag{C-6}$$

where $\bar{V}$ was calculated by the continuity equation

$$\bar{V} = M_L / \rho_L A_{NOZ} \tag{C-7}$$

using the measured flow rate M_L and the measured nozzle exit area A_{NOZ}. Equation C-4 may then be rewritten, in terms of ϕ and P_{DYN}'. Thus

$$\overline{P_{DYN}} = \frac{2P_{DYN}'}{R^2} \int_0^R r \, \phi \, dr \tag{C-8}$$

Figures C-2, C-3, and C-4 present the total pressure ratio ϕ as a function of the distance from the center of the jet r, as determined experimentally, for Nozzles 1, 2, and 3, respectively.

To integrate equation C-8 analytically, the functional relationship between ϕ and r is needed. For the purpose at hand, a power law relationship was employed. Thus

$$\phi = \phi_{MAX} (1 - r/R)^p \tag{C-9}$$

For each nozzle the value of p was chosen, by trial and error, for which the power law curve most closely approximated the experimental plot of ϕ as a function of r. Since the experimental total pressure readings were believed to be more accurate near the center of the stream, more emphasis was placed on fitting the calculated curve to the experimental data in that region. Figures C-2, C-3, and C-4 present the resulting power law relationships and curves for Nozzles 1, 2, and 3, respectively.

Substituting equation C-9 into equation C-8 and integrating,

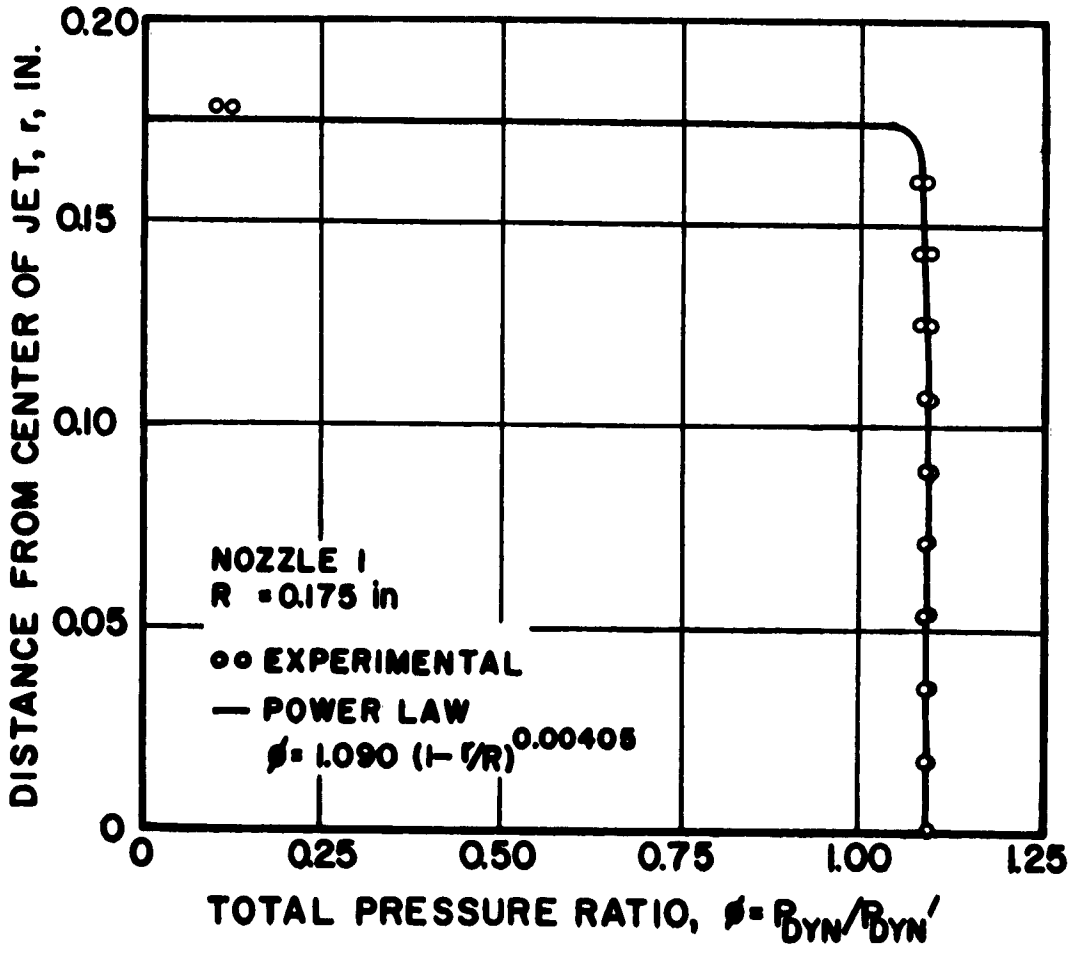

Fig. C-2 Total Pressure Ratio as a Function of the Distance from the Center of the Free Jet for Nozzle 1

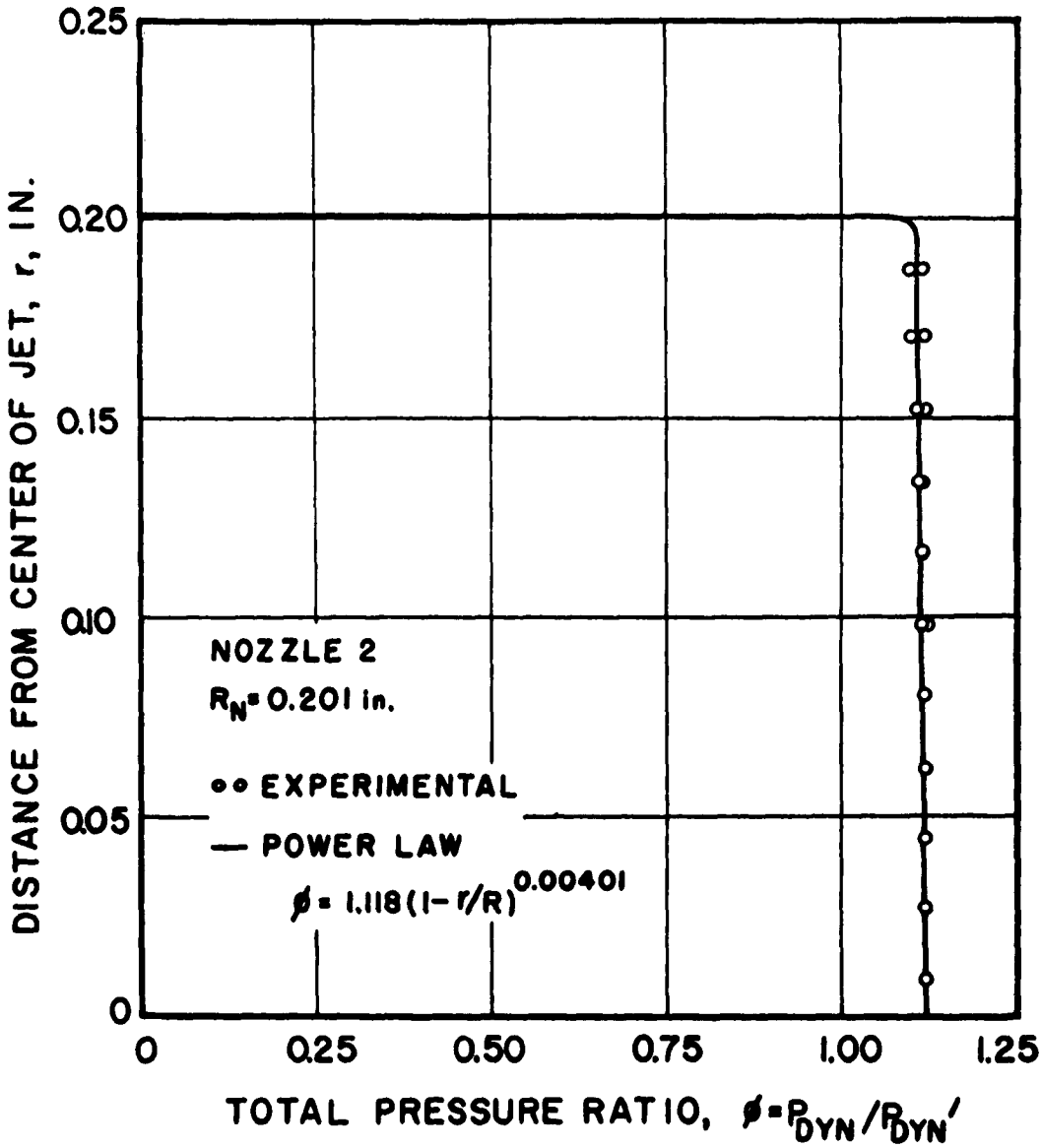

Fig. C-3 Total Pressure Ratio as a Function of the Distance from the Center of the Free Jet for Nozzle 2

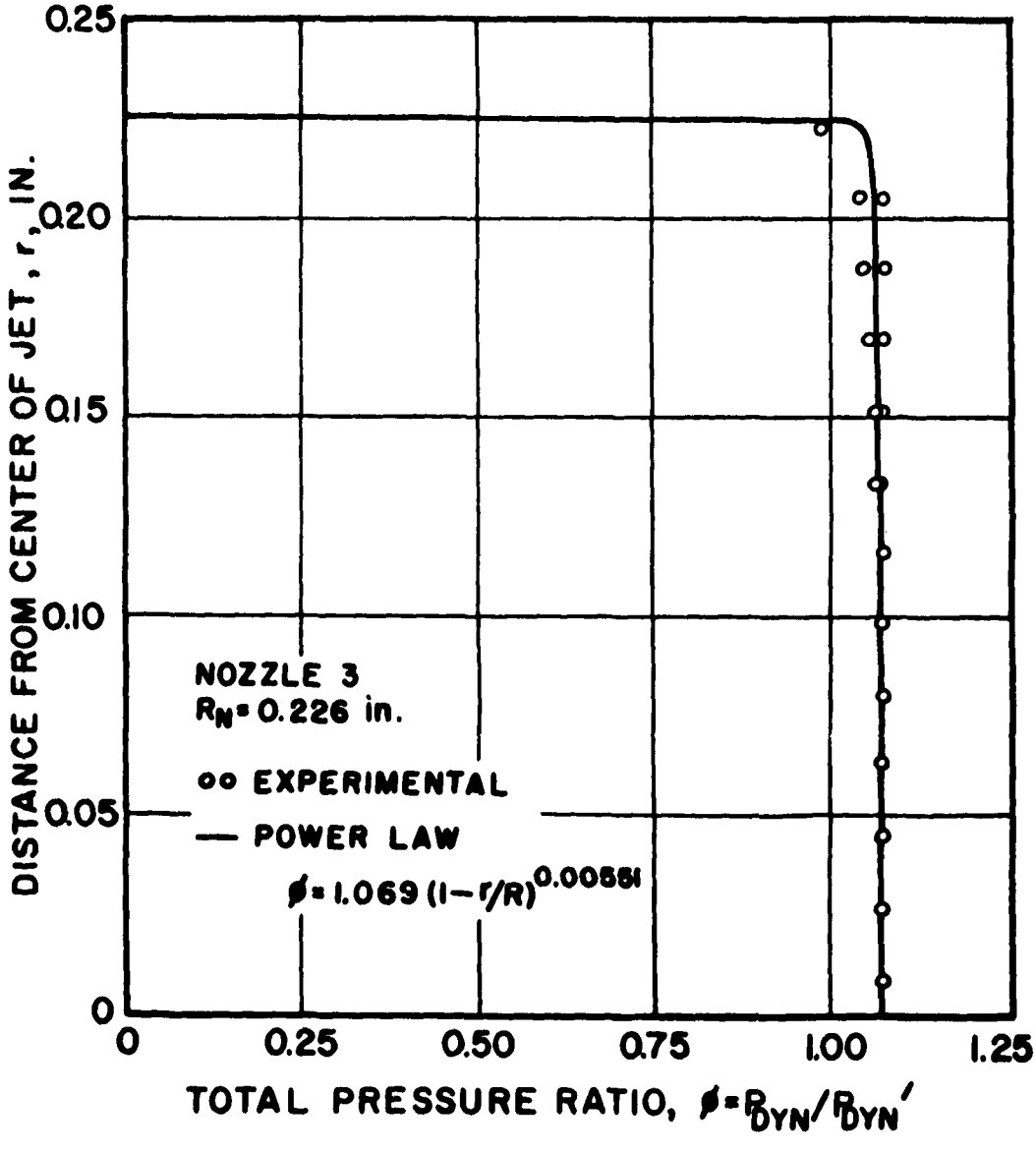

Fig. C-4 Total Pressure Ratio as a Function of the Distance from the Center of the Free Jet for Nozzle 3

yields

$$\overline{P_{DYN}} = P_{DYN}' \, \phi_{MAX} \, \frac{2}{(p+1)(p+2)} \qquad \text{(C-10)}$$

C-4 Results

When the appropriate values of ϕ_{MAX} and p for a given nozzle are substituted into equation C-10, the ratio of $\overline{P_{DYN}}$ to P_{DYN}' is obtained. Table C-1 presents $\overline{P_{DYN}}/P_{DYN}'$ for Nozzles 1, 2, and 3.

Table C-1

Ratio of the Mean Dynamic Pressure to the Nominal Dynamic Pressure for Nozzles 1, 2, and 3

Nozzle	$\overline{P_{DYN}}/P_{DYN}'$
1	1.084
2	1.111
3	1.060

The results presented in Table C-1 were employed in the Series II free-jet experiments by (1) calculating P_{DYN}' from measurements of M_L and A_{NOZ}, and (2) multiplying P_{DYN}' by the appropriate value of $\overline{P_{DYN}}/P_{DYN}'$.

C-5 Sources of Error

The two primary sources of error in the experiments described in this appendix, are (1) inaccuracies in the measured values of the dynamic pressure, especially near the outer edge of the jet, and (2) errors introduced by the discrepancies between the experimental data and the power law relationship.

APPENDIX D

THEORETICAL EFFICIENCY OF A TWO-PHASE DIFFUSER

D-1 Introduction

This appendix presents the derivation of the equations for calculating the diffuser efficiency K_D for the flow of a two-phase mixture of a liquid and a gas through a diverging diffuser.

Figure D-1 is a schematic diagram of a two-phase diverging diffuser. Station 1 is the entrance, or throat, cross-section of the diffuser, and station 2 is the exit cross-section of the diffuser, corresponding to the plenum chamber of the experimental diffusers.

D-2 Assumptions

The assumptions presented below were employed in the analysis of the two-phase diffuser.

(1) The flow is steady, frictionless, and one-dimensional.

(2) The gas and the liquid are uniformly mixed and travel at the same velocity.

(3) No heat is transferred across the boundaries of the diffuser.

(4) No external work is performed by the two-phase mixture.

(5) The only forces acting on the two-phase mixture are pressure forces.

(6) There are no changes in potential energy due to elevation changes.

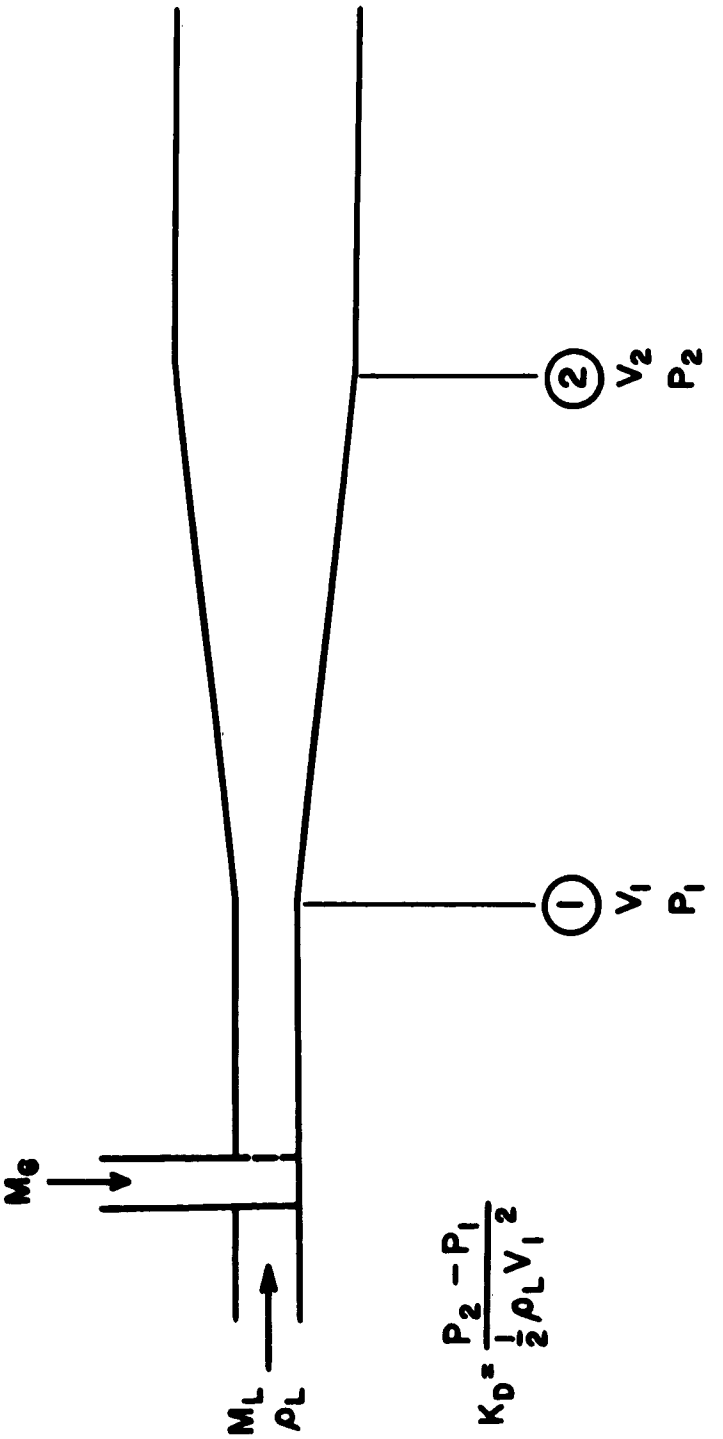

Fig. D-1 Schematic Diagram of a Two-Phase Diverging Diffuser

(7) The gas is perfect and has constant specific heats.

(8) The liquid is incompressible, has a constant specific heat, and has no vapor pressure.

(9) The kinetic energy leaving the diffuser is small compared with that entering the diffuser.

(10) The mass rate of flow of the gas is small compared with that of the liquid.

(11) The temperature of the gas remains equal to that of the liquid as the two-phase mixture flows through the diffuser.

D-3 Notation

At the entrance to the diffuser, station 1, let R_G denote the gas constant, C_p the specific heat of the gas, k its specific heat ratio, ρ_G the density of the gas, M_G the mass rate of flow of gas, ρ_L the density of the liquid, C_L its specific heat, and M_L the mass rate of flow of liquid. Assume that the gas and liquid are thoroughly mixed at station 1, and the temperature, pressure, and velocity of the two-phase mixture are T_1, P_1, and V_1, respectively.

Let u denote specific internal energy, s specific entropy, and h specific enthalpy; the subscripts G and L attached to those symbols denote gas and liquid, respectively. Let S denote the entropy of the two-phase mixture.

D-4 Derivation of Equations for Diffuser Efficiency

In view of assumptions 1 through 6, the steady flow energy equation, applied between stations 1 and 2, yields

$$M_G \left(u_{G2} - u_{G1} + \frac{P_2}{\rho_{G2}} - \frac{P_1}{\rho_{G1}} + \frac{V_2^2 - V_1^2}{2}\right)$$

$$+ M_L \left(u_{L2} - u_{L1} + \frac{P_2 - P_1}{\rho_L} + \frac{V_2^2 - V_1^2}{2}\right) = 0 \qquad \text{(D-1)}$$

which may be rewritten as

$$\frac{P_2 - P_1}{\rho_L} = \frac{M_G}{M_L}\left(u_{G1} - u_{G2} + \frac{P_1}{\rho_{G1}} - \frac{P_2}{\rho_{G2}} + \frac{V_1^2 - V_2^2}{2}\right) + u_{L1} - u_{L2} + \frac{V_1^2 - V_2^2}{2}$$

(D-2)

Dividing equation D-2 by $(V_1^2 - V_2^2)/2$, and noting that by virtue of assumption 7

$$u_G + \frac{P}{\rho_G} = h_G = C_P T_G$$

substitute for u_G in equation D-2, yielding

$$\frac{P_2 - P_1}{\frac{1}{2}\rho_L (V_1^2 - V_2^2)} = 1 + \frac{M_G}{M_L}\left(1 + \frac{2C_P (T_{G1} - T_{G2})}{V_1^2 - V_2^2}\right) + \frac{2 (u_{L1} - u_{L2})}{V_1^2 - V_2^2} \qquad \text{(D-3)}$$

Since the kinetic energy of a fluid is proportional to the square of its velocity, assumption 9 yields

$$V_1^2 - V_2^2 \approx V_1^2$$

By definition, the diffuser efficiency K_D is given by

$$K_D = (P_2 - P_1)/\tfrac{1}{2}\rho_L V_1^2$$

It follows that

$$K_D = 1 + \frac{M_G}{M_L}\left(1 + \frac{2C_P\,(T_{G1} - T_{G2})}{V_1^2}\right) + \frac{2\,(u_{L1} - u_{L2})}{V_1^2} \qquad \text{(D-4)}$$

From assumption 11, it is seen that $T_G = T_L = T$. Examine the last term in equation D-4. For the liquid component $\Delta u_L = C_L \Delta T$, so that

$$u_{L1} - u_{L2} = C_L\,(T_1 - T_2) \qquad \text{(D-5)}$$

Substituting equation D-5 into equation D-4, yields

$$K_D = 1 + \frac{M_G}{M_L}\left(1 + \frac{2C_P\,(T_1 - T_2)}{V_1^2}\right) + \frac{2\,C_L\,(T_1 - T_2)}{V_1^2} \qquad \text{(D-6)}$$

Employing assumption 10, it is noted that

$$\frac{M_G}{M_L}\,\frac{2C_P\,(T_1 - T_2)}{V_1^2} \ll \frac{2\,C_L\,(T_1 - T_2)}{V_1^2} \qquad \text{(D-7)}$$

Hence, the expression on the left-hand side of inequality D-7 may be neglected in equation D-6 without introducing appreciable error. Thus, equation D-6 reduces to

$$K_D = 1 + \frac{M_G}{M_L} + \frac{2\,C_L\,(T_1 - T_2)}{V_1^2} \qquad \text{(D-8)}$$

Since the gas and the liquid remain at the same temperature as the two-phase mixture flows through the diffuser, any transfer of heat from the gas to the liquid is reversible. Since the flow of the mixture is

adiabatic and frictionless, there is no change in the entropy of the mixture, or

$$\Delta S = 0 \tag{D-9}$$

The change in the specific entropy of the gas between stations 1 and 2 is given by

$$\Delta s_G = C_P \ln \frac{T_2}{T_1} - R_G \ln \frac{P_2}{P_1} \tag{D-10}$$

The change in the specific entropy of the liquid between stations 1 and 2 is given by

$$\Delta s_L = C_L \ln \frac{T_2}{T_1} \tag{D-11}$$

Since

$$\Delta S = M_G \Delta s_G + M_L \Delta s_L$$

it follows from equations D-9, D-10, and D-11, that

$$M_G \left(C_P \ln \frac{T_2}{T_1} - R_G \ln \frac{P_2}{P_1}\right) + M_L C_L \ln \frac{T_2}{T_1} = 0 \tag{D-12}$$

Solving equation D-12 for T_2/T_1, yields

$$\frac{T_2}{T_1} = \left(\frac{P_2}{P_1}\right)^{\frac{R_G M_G/M_L}{C_P M_G/M_L + C_L}} \tag{D-13}$$

Based on assumption 10, the right hand side of equation D-13 may be approximated by the first two terms of its exponential series expansion. Thus

$$\frac{T_2}{T_1} = 1 + \frac{R_G M_G/M_L}{C_P M_G/M_L + C_L} \ln \frac{P_2}{P_1} \qquad \text{(D-14)}$$

Equation D-14 may be further simplified by noting that assumption 10 yields

$$C_P M_G/M_L + C_L \approx C_L \qquad \text{(D-15)}$$

Substituting equation D-15 into equation D-14 and rearranging, yields

$$T_2 - T_1 = \frac{R_G T_1}{C_L} \frac{M_G}{M_L} \ln \frac{P_2}{P_1} \qquad \text{(D-16)}$$

Combining equations D-8 and D-16, gives

$$K_D = 1 + \frac{M_G}{M_L}\left(1 - \frac{2 R_G T_1}{V_1^2} \ln \frac{P_2}{P_1}\right) \qquad \text{(D-17)}$$

Equation D-17 is an approximate expression for the diffuser efficiency for isentropic two-phase flow with no internal temperature difference. It cannot be solved explicitly for K_D, but can be solved by iteration.

"Distribution of this report has been made in accordance with the Joint Army-Navy-Air Force Liquid Propellant Mailing List of March 1962."